



CrossMark  
 click for updates

Cite this: *RSC Adv.*, 2017, 7, 10021

# Promising advances of thiacalix[4]arene in crystal structures

Mei Zhao, Jing Lv and Dian-Shun Guo\*

Thiacalix[4]arenes are one kind of robust scaffolds and extensively applied in supramolecular chemistry and materials science owing to their novel features. This article reviews the research progress of thiacalix[4]arene derivatives in crystal and organic supramolecular structures. The actual morphological parameters of various conformers and their binding patterns as well as typical supramolecular assemblies are briefly summarized. Versatile interactions involving hydrogen bonds, C–H $\cdots$  $\pi$ ,  $\pi$ – $\pi$ , halogen $\cdots$  $\pi$  and ancillary electrostatic contacts between heteroatoms were found to play an important role in governing the conformational and supramolecular structures of thiacalix[4]arenes in the solid state. In some cases, the solvent molecules also participate in regulating the conformer and the packing of thiacalix[4]arenes.

Received 21st October 2016  
 Accepted 19th January 2017

DOI: 10.1039/c6ra25616c

[www.rsc.org/advances](http://www.rsc.org/advances)

## 1. Introduction

Thiacalix[4]arenes, new members of the calixarene family,<sup>1,2</sup> have now become one kind of robust scaffolds and have attracted considerable attention in supramolecular chemistry and materials science.<sup>3–14</sup> Compared with calix[4]arene, the four S bridges replacing the CH<sub>2</sub> linkers endow many novel features such as larger cavity, better flexibility, richer conformational behavior, and the possibility of multiple chemical modifications.<sup>5</sup> Moreover, the introduction of S atoms makes thiacalix[4]arenes possess the additional affinity for binding desired substrates in their supramolecular systems.

Thiacalix[4]arenes, as versatile building blocks for highly organized receptors, have attracted much interest for more than two decades largely because of their specific affinity and selectivity in molecular recognition,<sup>6–9</sup> and supramolecular assembly.<sup>10–14</sup> Meanwhile, great advances have also been made to describe the precise morphology of various conformers and binding patterns of thiacalix[4]arene derivatives in the solid state, which are difficult to accurately deal with in solution owing to the flexibility of the thiacalix[4]arene platform. The crystal structures of thiacalix[4]arene derivatives as important ligands in coordination chemistry have been highlighted in recent reviews.<sup>11,12</sup> However, as of now, the progress of thiacalix[4]arene derivatives in the crystal structures and organic supramolecular assemblies has not been reviewed. This article is intended to summarize the major advances in this field, according to cone, 1,3-alternate, 1,2-alternate and partial cone conformers (Fig. 1), respectively.

College of Chemistry, Chemical Engineering and Materials Science, Collaborative Innovation Center of Functionalized Probes for Chemical Imaging in Universities of Shandong, Shandong Normal University, Jinan 250014, P. R. China. E-mail: [chdsguo@sdnu.edu.cn](mailto:chdsguo@sdnu.edu.cn); Fax: +86 531 86928773; Tel: +86 531 86180743



*Mei Zhao received her MS degree in organic chemistry from Shandong Normal University. She has been working in Shandong Analysis and Test Center since 2009. Currently, she is pursuing her PhD at Shandong Normal University under the supervision of Prof. Dian-Shun Guo. Her research interest is focused on the development of new optical- and redox-active sensors based on thiacalix[4]arenes and their applications.*



*Jing Lv is working for her MS degree at Shandong Normal University under the supervision of Prof. Dian-Shun Guo. She completed her BSc degree in chemistry at Shandong Normal University in 2014. Her current research interest is concentrated on the development of novel optical and redox active multiple sensors.*



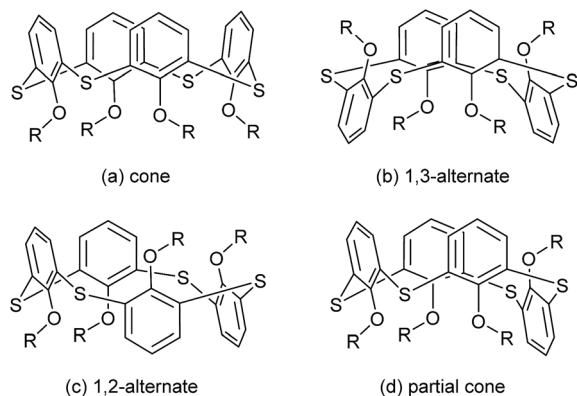


Fig. 1 Four main conformers of thiacalix[4]arene: (a) cone, (b) 1,3-alternate, (c) 1,2-alternate, and (d) partial cone.

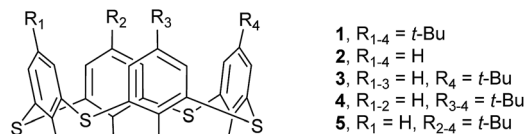
In this review, we will focus on the precise conformations, binding patterns, and some typical supramolecular assemblies of thiacalix[4]arene derivatives mainly found in the solid state. The exactly conformational shape of thiacalix[4]arene core is characterized with the dihedral angles (termed as  $\theta$ , interior angle) between the phenolic rings and the virtual plane ( $R$ ) defined by the four S bridges. The difference amongst  $\theta$  angles is significant for the shape of the thiacalix[4]arene core, the bigger the  $\theta$  range, the more distorted the conformation.

## 2. Cone structures of thiacalix[4]arenes

Thiacalix[4]arenes in a cone conformation are easily available, thus many crystal structures of such conformers are proved by X-ray diffraction analysis. In this section, they will be discussed mainly according to the  $O$ -substituted extent at the lower rim.

### 2.1 Parent thiacalix[4]arenes and their analogues

As demonstrated by Miyano *et al.*,<sup>3</sup> the parent *p-t*-butylthiacalix[4]arene **1** (Fig. 2) shows very simple <sup>1</sup>H NMR spectra in solution. Although the <sup>1</sup>H NMR chemical shift for the OH groups of **1** suggested the formation of intramolecular H-bonds, their



- 1,  $R_{1-4} = t\text{-Bu}$
- 2,  $R_{1-4} = \text{H}$
- 3,  $R_{1-3} = \text{H}, R_4 = t\text{-Bu}$
- 4,  $R_{1-2} = \text{H}, R_{3-4} = t\text{-Bu}$
- 5,  $R_1 = \text{H}, R_{2-4} = t\text{-Bu}$

Fig. 2 Structures of compounds 1–5.

actual morphology is difficult to give. Alternatively, in the solid state, the parameters of a conformer can be exactly described by the X-ray diffraction analysis. And the shape of the thiacalix[4]arene core can be characterized by the  $\theta$  angles.<sup>15</sup> The crystal structure of **1** (Fig. 3) shows a perfect  $C_4$ -symmetric cone conformation identified by the same  $\theta$  value of  $119.0^\circ$  (Table 1).<sup>16</sup> This may be ascribed to the formation of an intramolecular cyclic hydrogen bonding array involving four identical  $\text{O-H}\cdots\text{O}$  H-bonds between the phenolic OH groups.<sup>17</sup>

The skeleton of **1** is flexible enough to preorganize and include various small organic molecules into its cavity forming inclusion crystals.<sup>18–21</sup> It was found that molecule **1** still retains a perfect  $C_4$ -symmetric structure when some small organic molecules incorporated into its cavity, while it will adopt a slightly distorted conformation upon inclusion of some bigger molecules. This tailors the need for producing stable crystals through conformational interchanges between host and guest molecules. For instance, the cone conformer of **1** in complex **1**·DCE (DCE is 1,2-dichloroethane, a bigger molecule) is slightly distorted, with different  $\theta$  values of  $125.9, 118.7, 136.5$  and  $124.1^\circ$ .<sup>18</sup> When MeCN (a smaller molecule) is included into the cavity of **1**, it still keeps the perfect  $C_4$  symmetry (Fig. 3).<sup>20</sup> The Me group of MeCN directs inside the cavity and its C–H bonds are perpendicular to the aromatic rings, where  $\text{C-H}\cdots\pi$  contacts exist to stabilize the complex **1**·MeCN. Moreover, the CN lobe of MeCN connects to the lower rim of the vicinal molecule **1** by  $\text{O-H}\cdots\text{N}$  H-bonds. Thus a head-to-tail type of infinite columnar structure is created by these interactions.

Compounds 2–5 (Fig. 2),<sup>16,22</sup> various de-*t*-butylation derivatives of **1**, all adopt a cone conformation (Fig. 4). However, they



Dian-Shun Guo is currently a Professor of organic chemistry at Shandong Normal University. He obtained his PhD in 1999 at Nankai University and worked as a Postdoctoral Research Associate with Prof. Wei-Min Dai at Hong Kong University of Science & Technology between 2000 and 2003. His current research is on the development of advanced materials involving thiacalix[4]arenes, optical probes and electrochemical sensors.

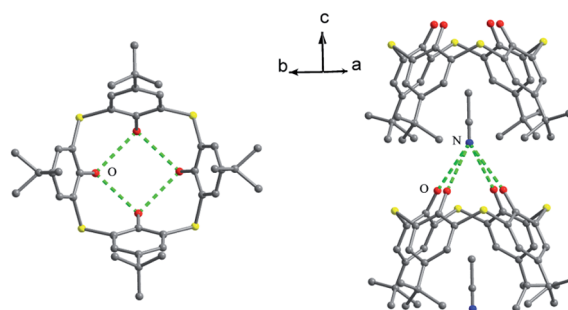


Fig. 3 Crystal structure (left) and partial packing structure (right) of **1** with MeCN in a head-to-tail manner. All protons of the OH groups were not found in their crystal. Note: all H atoms not involving weak interactions (mapped with various colour dashed lines) and minor disordered atoms (if any) are omitted for clarity in all crystal structures discussed in this review.



Table 1 The  $\theta$  angles of compounds 1–46<sup>a</sup>

Compd.	$\theta$ (°)			
1	119.0	119.0	119.0	119.0
2	114.4	136.9	117.8	136.9
3A	108.2	142.9	111.4	143.2
3B	107.9	144.5	108.7	139.8
4	100.0	141.4	112.1	146.3
5	120.4	133.1	130.1	126.7
6	115.7	126.2	121.1	126.0
7	123.3	123.3	123.3	123.3
8	108.1	142.2	120.3	132.6
9	112.0	112.6	112.0	112.6
10	115.7	115.7	115.7	115.7
11	103.6	125.8	103.6	125.8
12	60.0	139.3	120.5	139.5
13	65.5	139.8	129.8	133.6
14A	66.2	148.1	116.4	139.3
14B	65.5	149.3	116.4	138.9
15	108.2	128.3	112.2	122.0
16	68.9	125.9	137.3	139.8
17	104.7	147.0	106.3	146.4
18	92.9	148.7	111.6	143.6
20	86.5	147.9	62.2	154.2
21	112.1	123.5	115.5	131.1
22	71.2	146.2	102.4	147.3
23	74.3	135.1	103.0	140.0
24A	69.9	140.1	109.2	135.6
24B	71.3	138.4	115.2	134.7
25	77.0	133.4	108.8	124.1
26	68.3	139.5	108.2	138.1
27A	93.0	136.4	96.6	138.6
27B	94.3	135.5	102.1	138.2
28	71.0	157.4	109.2	143.1
29	108.8	149.4	109.7	144.3
30	106.5	142.1	108.9	146.5
31	102.9	135.6	114.1	147.3
32	111.3	136.0	111.3	136.0
33	69.8	159.3	70.8	151.6
34A	54.3	104.3	43.1	75.7
34B	41.5	94.0	51.9	87.5
35	79.2	126.7	95.8	141.1
36	78.7	121.3	91.5	123.8
37	65.2	136.0	65.4	136.7
38	106.0	108.2	115.0	116.9
39 <sup>b</sup>	67.5	146.5	69.2	146.0
40	92.6	131.7	93.1	126.3
41	90.2	128.8	91.5	132.8
42	90.3	130.6	96.0	132.5
43	87.4	142.8	91.2	140.8
44	75.0	141.9	107.0	143.5
45	65.6	139.7	81.2	153.9
46	106.7	134.9	110.9	132.0

<sup>a</sup> Data obtained by calculation with Diamond Version 3.0. <sup>b</sup> Data obtained from refs.

exhibit two different modes: one has near  $C_2$  symmetry (2, 3 and 4), and the other shows near  $C_4$  symmetry (5), with four varied  $\theta$  angles (Table 1). In the conformers of 2–4, O atoms of the OH groups are not arranged on one plane but deviate up and down, which would obstruct the formation of the intramolecular cyclic H-bonded array. Especially in 4, such tendency appears clearly with disappearance of the circular O–H...O H-bonds (Fig. 4c), due to the asymmetrical situations of the *p*-substituted groups.

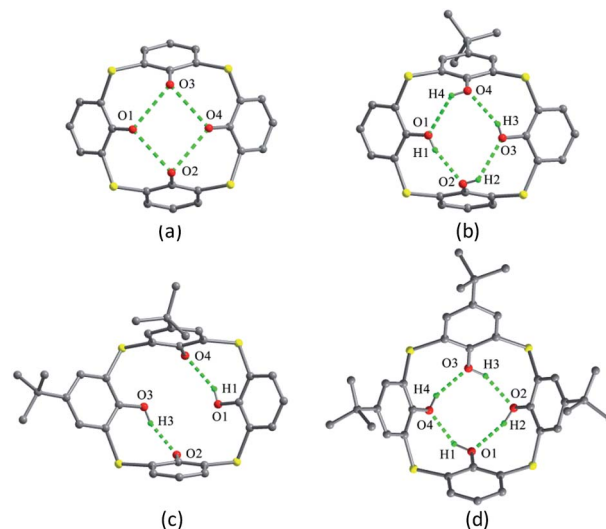


Fig. 4 Crystal structures of 2 (a), 3 (b), 4 (c) and 5 (d). All protons of the OH groups were not found in the crystal of 2.

On the other hand, for 2, 3 and 5, the cyclic H-bonded array is remained (Fig. 4).

In the packing, a self-inclusion trimer of 2 is formed by C–H... $\pi$  interactions, owing to removal of all four *t*-butyl groups (Fig. 5a). In the cases of 3–5, all give self-inclusion dimers in such a manner that the phenolic moiety of one molecule is inserted into the cavity of the other one. In 3 (Fig. 5b) and 4 (Fig. 5c), the phenolic rings with *t*-butyl-free are inserted into each other with face-to-face  $\pi$ – $\pi$  interactions. In 5 (Fig. 5d), a *t*-butyl group enters into the cavity, accompanied by some C–H... $\pi$  interactions. Moreover, these dimers in 3–5 further associate each other by the face-to-face overlap between the *t*-butyl-free phenol rings.

Thiacalix[4]arene 6 (Fig. 6),<sup>23</sup> with four phenyl groups at the upper rim, adopts a cone conformation with four different  $\theta$  values (Table 1). This conformer is also governed by the intramolecular cyclic H-bonding array at the lower rim, creating

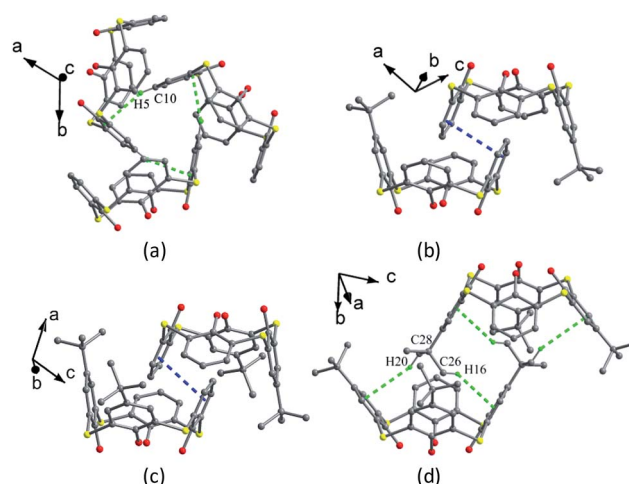


Fig. 5 Partial packing structures of 2 (a), 3 (b), 4 (c) and 5 (d).



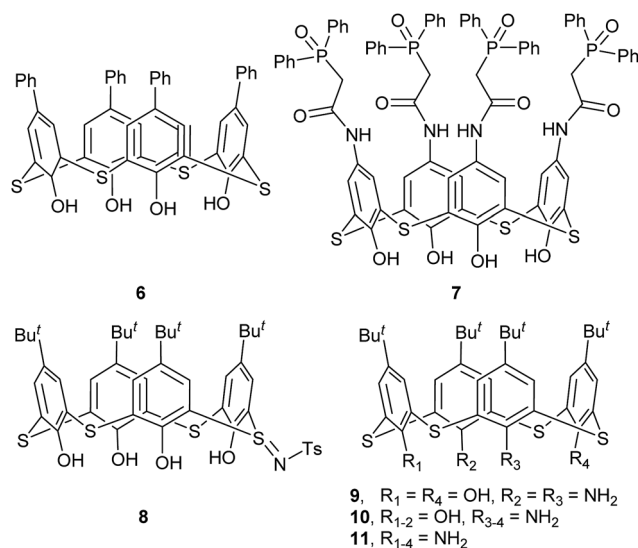


Fig. 6 Structures of compounds 6–11.

a deeper cavity (Fig. 7a). Such a deep-cavity thiacalix[4]arene possesses an extended  $\pi$ -aromatic system, and is potentially useful for solid state inclusion of suitable molecules.

Thiacalix[4]arene **7** (Fig. 6),<sup>24</sup> with four CMPO (carbamoylmethylphosphineoxide) units at the upper rim, shows a perfect cone conformation with the same  $\theta$  value of 123.3°. In its crystal structure (Fig. 7b), the typical circular hydrogen bonding array is also found, indicating that the CMPO units are large but cannot disrupt the H-bonded array formation. In the stacking (Fig. 8), the CMPO moieties of two molecules are interlocked to create a capsule-like dimer with  $S_8$  symmetry by intermolecular N–H $\cdots$ O H-bonds between the CONH and P=O groups. This capsule-like dimer can exist in apolar solvents and be applied for inclusion of some guests in solution.

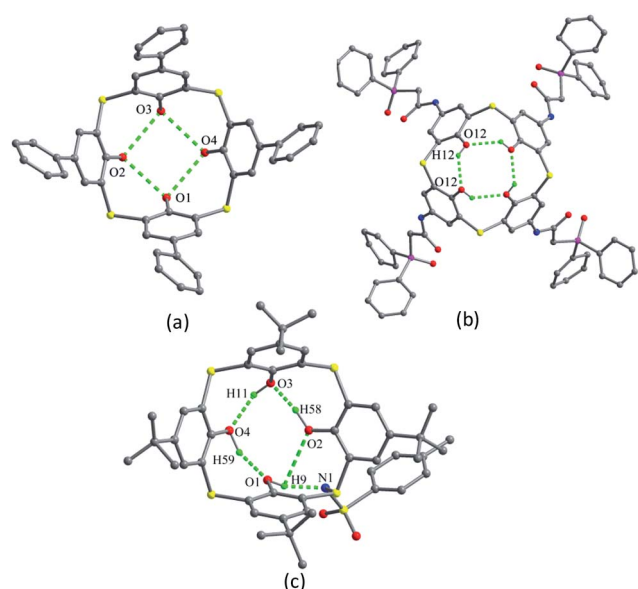


Fig. 7 Crystal structures of **6** (a), **7** (b) and **8** (c), showing the circular H-bonding array.

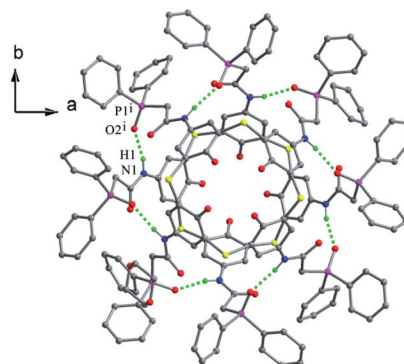


Fig. 8 A dimeric capsule of **7**, showing intermolecular H-bonds.

Compound **8** (ref. 25) (Fig. 6) is a derivative of **1** with a S bridge modified by sulfilimine moiety, and takes a distorted cone conformation with four different  $\theta$  values (Table 1), in which the sulfilimine group directs toward the axial orientation (Fig. 7c). This conformer is stabilized by an intramolecular cyclic H-bonded array and an O1–H9 $\cdots$ N1 H-bond between one OH group and N atom of the sulfilimine unit.

Thiacalix[4]arene analogues **9** and **10** (Fig. 6),<sup>26</sup> with two amino groups at the lower rim, are also in a cone conformation with a circular H-bonded array in their crystals (Fig. 9a and b). However, the averaged distance between adjacent N, O atoms of **9** and **10** falls in the order of O $\cdots$ O < O $\cdots$ N < N $\cdots$ N, revealing that the strength of intramolecular H-bonds is weaker than those of **1**. For this reason, thiacalix[4]arene analogue **11** (Fig. 6), with four NH<sub>2</sub> groups, takes in either a cone or a 1,3-alternate conformation based on inclusion with different solvent molecules.<sup>27,28</sup> It adopts a  $C_2$  cone conformation when a MeCN molecule is included into its cavity with two pairing  $\theta$  angles of 103.6 and 125.8°, resulting from the co-operation of intramolecular N–H $\cdots$ N and N–H $\cdots$ S H-bonds (Fig. 9c), as well as intermolecular N–H $\cdots$ N H-bonds with MeCN molecule (Fig. 9d). Whereas, it takes a 1,3-alternate conformation when a CH<sub>2</sub>Cl<sub>2</sub> molecule occupies its cavity with two pairs of  $\theta$  values (100.2 and 112.4°) as they only form weak C–H $\cdots$  $\pi$  contacts (Fig. 9e). In the case of guest-free, **11** shows a typical 1,3-alternate conformer with the same  $\theta$  value of 95.3°, creating eight intramolecular N–H $\cdots$ S H-bonds (Fig. 9f).

## 2.2 O-Monosubstituted thiacalix[4]arenes

The chemical modification of the OH groups at the lower rim of thiacalix[4]arenes by selective etherification or esterification could provide mono- to tetra-*O*-substituted thiacalix[4]arene derivatives with some novel features.

Compounds **12–14** (Fig. 10), mono etheral derivatives of **1**, all display a pinched cone conformation typically with four different  $\theta$  angles (Table 1). The substituted phenolic ring is almost parallel to its opposite one and forms the smallest  $\theta$  angle with the *R* plane. In **12** (Fig. 11a),<sup>29</sup> such a conformer is fixed by intramolecular sequential O–H $\cdots$ O H-bonds between OH groups. Additionally, an intramolecular C–H $\cdots$ O H-bond between the P(O)CH<sub>2</sub>O moiety and one neighboring OH group





out with  $\theta$  values of 139.8 and 125.9°, while the other benzene rings are pinched with  $\theta$  values of 68.9 and 137.3°. Similar to **13**, the thiacalix[4]arene core is very distorted with the middle phenolic ring bent outwards the cavity, resulting from H-bonds between O<sup>-</sup> and two adjacent OH groups (Fig. 13a). In addition, the asymmetric unit comprises one thiacalix[4]arene molecule, one methanol and two waters of crystallization, in which H-bonds between them are further to stabilize the conformer.

Thiacalix[4]arene derivatives **17** and **18** (Fig. 12),<sup>34,35</sup> with one decyloxy group at the lower rim, give a similarly flattened cone conformation with  $\theta$  ranges of 104.7–147.0° and 92.9–148.7° (Table 1), respectively. Although either conformer is governed by three intramolecular H-bonds, the H-bonding patterns are different: the former created in a sequential way from one OH group to the ether O atom (Fig. 13b), while the latter yielded in such a way that one ether O atom forms two H-bonds with its vicinal OH groups (Fig. 13c).

Lhoták *et al.* synthesized a phenoxanthiin-containing thiacalix[4]arene **19** (Fig. 14).<sup>36</sup> It takes a cone conformer, where the S atom of phenoxanthiin ring makes a radical departure from the other S bridges. Such a structure is supported by an intramolecular circular array of H-bonds between the three OH groups. This bonding array is further strengthened by H-bonds between the S bridges and the adjacent OH groups. In addition, it crystallizes with two CH<sub>2</sub>Cl<sub>2</sub> molecules, one of which is situated directly inside the calix cavity, with Cl atom located above the centre of one phenolic ring with a distance of 3.31 Å, indicating the presence of Cl⋯ $\pi$  interaction.

### 2.3 O-Disubstituted thiacalix[4]arenes

Most disubstituted derivatives of thiacalix[4]arene could be easily obtained in their 1,3-diethers with two free OH groups. Usually, they show a pinched cone conformation with a couple of opposite benzene rings tilting to the same orientation.

Compounds **20** and **21** (Fig. 15),<sup>37</sup> diacetate derivatives of thiacalix[4]arene and calix[4]arene respectively, have distinct

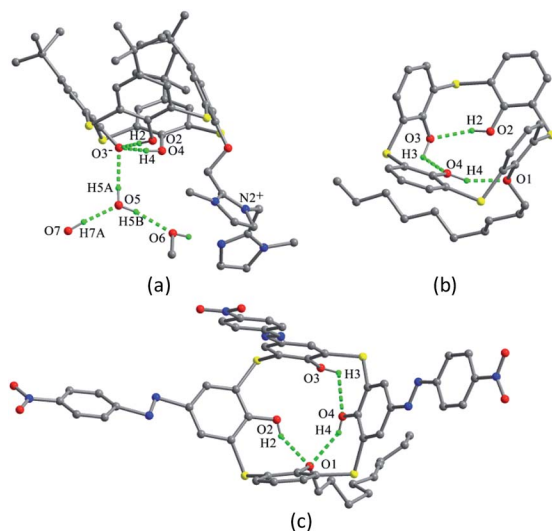


Fig. 13 Crystal structures of **16** (a), **17** (b) and **18** (c), showing different H-bonds.

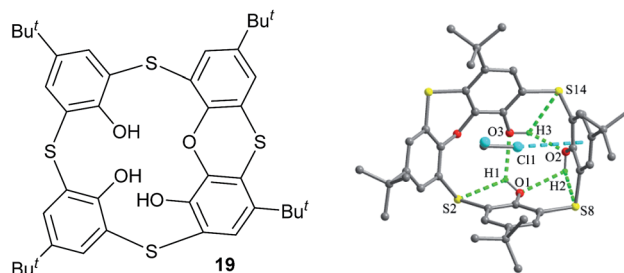


Fig. 14 Chemical and crystal structures of compound **19**, showing intramolecular H-bonding array and intermolecular Cl⋯ $\pi$  interaction.

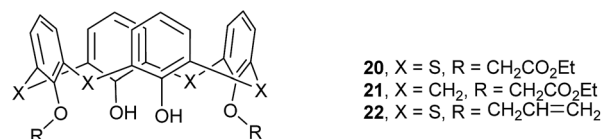


Fig. 15 Structures of compounds **20–22**.

conformational behavior owing to the different H-bonding patterns. In the crystal structure of **20** (Fig. 16a), the distorted cone conformer, with different  $\theta$  values of 86.5, 147.9, 62.2 and 154.2°, is governed by two intramolecular H-bonds from both OH groups to the same ether O atom. This asymmetrical arrangement of H-bonds decreases the overall symmetry. However, in the case of **21** (Fig. 16b), two free OH groups interact with the different ether O atoms, producing almost symmetrical intramolecular H-bonds and giving a nearly C<sub>2</sub>-symmetric cone conformation with  $\theta$  values of 112.1, 123.5, 115.5 and 131.1°. This difference could be ascribed to the size of the thiacalix[4]arene cavity larger (15%) than that of the calix[4]arene.<sup>16</sup>

Thiacalix[4]arene diallylether **22** (ref. 38) (Fig. 15) adopts a pinched cone conformation with  $\theta$  values of 71.2, 146.2, 102.4 and 147.3°, in which one ether chain is bent towards the cavity. This conformer is fixed by the same intramolecular H-bonds as in **20** (Fig. 16c). In the packing, an infinite chain of **22** with alternating orientations is formed by the  $\pi$ - $\pi$  stacking between phenolic rings (Fig. 17).

Thiacalix[4]arene derivatives **23–26** (Fig. 18) all take a pinched cone conformation with similar  $\theta$  values from 68.3 to 140.1° (Table 1). The two opposing aromatic rings attaching

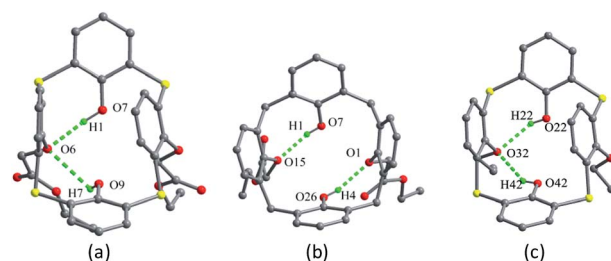


Fig. 16 Crystal structures of **20** (a), **21** (b) and **22** (c), showing intramolecular H-bonds.



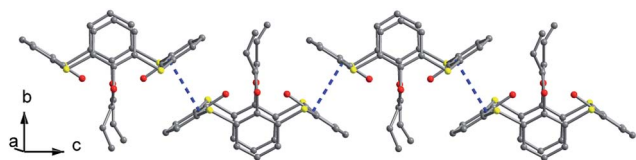


Fig. 17 An infinite chain of 22 built by  $\pi$ - $\pi$  stacking.

ether arm are almost parallel to each other, while two phenolic rings are tilted outwards and nearly perpendicular. The conformer of 23 (ref. 39) is fixed by the H-bonds as mentioned above, in which two opposite aromatic rings with  $\text{OCH}_2\text{CN}$  moiety tilt parallel to the same direction (Fig. 19a). Moreover, intramolecular  $\text{O}\cdots\text{S}$  H-bonds yielded between the OH groups and S bridges are the factor for stabilizing the conformation.

Thiocalix[4]arene diisocyanide derivative 24 (ref. 40) exists two molecules **A** and **B** in its crystal structure. In **A** (Fig. 19b), both  $\text{OCH}_2\text{CH}_2\text{N}\equiv\text{C}$  arms point vertically to two sides, while in **B** (Fig. 19c), both  $\text{OCH}_2\text{CH}_2\text{N}\equiv\text{C}$  arms point parallel to one side owing to the formation of an intramolecular  $\text{C}\cdots\text{C}$  H-bond between the two arms. Similarly, intramolecular  $\text{O}\cdots\text{H}$  H-bonds were also found between the OH groups and ether O atoms. In the packing (Fig. 20), an asymmetric dimer of molecule 24 is formed by an intermolecular  $\text{C90}\cdots\text{H90}\cdots\text{C46}$  interaction between vicinal molecules **A** and **B**. Then, each dimer is connected in turn to produce a 1-D **ABAB** type of chain by  $\text{C22}\cdots\text{H22}\cdots\text{O8}$  H-bonds. Moreover, this chain is further fixed by intermolecular  $\text{O4}\cdots\text{S5}$  and  $\text{C21}\cdots\text{H21}\cdots\pi$  contacts.

The conformer of 25 (Fig. 21a),<sup>40</sup> with two  $\text{OCH}_2\text{CH}_2\text{NH}_2$  arms, is also fixed by the intramolecular  $\text{O}\cdots\text{H}$  H-bonds from both OH groups to the same ether O atom. Interestingly, one aminoethyl group was disordered over two orientations, where

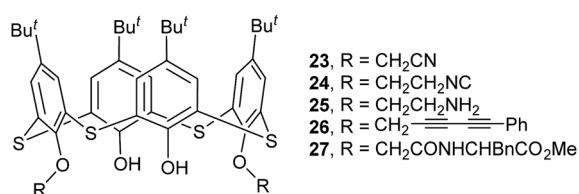


Fig. 18 Structures of compounds 23–27.

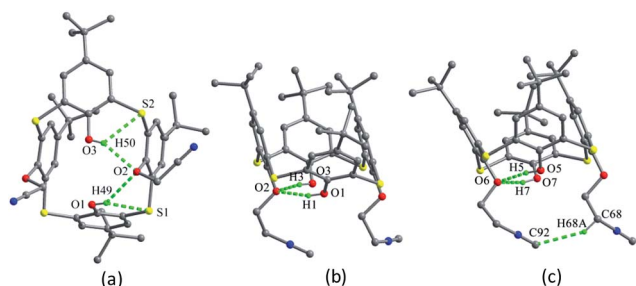


Fig. 19 Crystal structures of 23 (a), 24A (b) and 24B (c), showing intramolecular H-bonds.

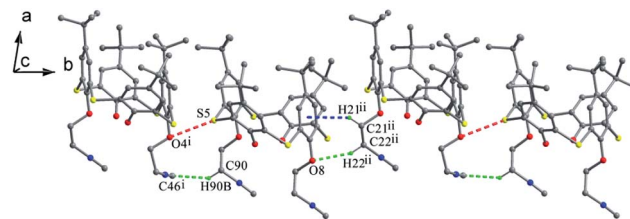


Fig. 20 A 1-D chain of 24, showing the  $\text{C}\cdots\text{H}\cdots\text{C}$  (green),  $\text{C}\cdots\text{H}\cdots\text{O}$  (green),  $\text{C}\cdots\text{H}\cdots\pi$  (blue) and  $\text{O}\cdots\text{S}$  (red) interactions.

three fifths of an intramolecular  $\text{N2}\cdots\text{H2}\cdots\text{O3}$  H-bond further governs the pinched cone conformation, while two fifths of an intermolecular  $\text{O1W}\cdots\text{H1D}\cdots\text{O3}$  H-bond occupies the site of  $\text{N2}\cdots\text{H2}\cdots\text{O3}$  when the aminoethyl unit is disordered over the other position. In the packing, six molecules of 25 combine in a sequential manner to construct a circular hexamer by cooperative intermolecular  $\text{C43}\cdots\text{H43}\cdots\pi$  and  $\text{S}\cdots\text{S}$  contacts (Fig. 22). Although compound 26 (ref. 41) possesses two longer chains, it still displays the similar conformational behavior (Fig. 21b), where two OH groups take part in H-bonds with the same ether O atom.

Thiocalix[4]arene derivative 27 (ref. 42) (Fig. 18) contains two ether arms with amide and ester groups at 1,3-position and can be applied for selective binding  $\text{Hg}^{2+}$  ion in acetonitrile solution. In the solid state, there are two molecules **A** and **B** in the asymmetric unit, both showing a cone conformation with near  $C_2$  symmetry (Table 1). Differently, two OH groups as a donor form  $\text{O}\cdots\text{H}\cdots\text{O}$  H-bonds not with the same ether O atom but with two O atoms (Fig. 21c). Moreover, each OH group also creates  $\text{O}\cdots\text{H}\cdots\text{O}$  and  $\text{N}\cdots\text{H}\cdots\text{O}$  H-bonds with the ester carbonyl O and NH atoms of the other ether strand, as well as  $\text{O}\cdots\text{H}\cdots\text{S}$  H-bond with the S bridge. The donor and acceptor capability of the OH groups with the ester carbonyl O and amide H formulates the orientation of the flexible arms upwards to the calix core direction. In addition, the terminal

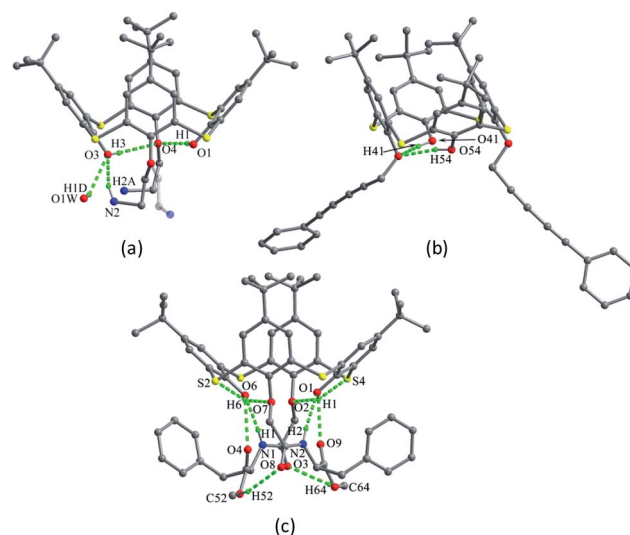


Fig. 21 Crystal structures of 25 (a), 26 (a) and 27 (c), showing H-bonds.



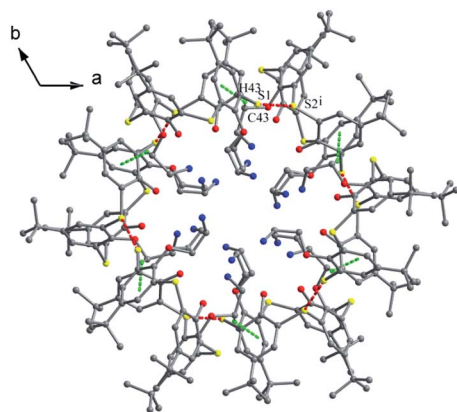


Fig. 22 An annular hexamer of **25** assembled by C–H... $\pi$  (green) and S...S (red) interactions.

methyl H of the ester group is involved in C–H...O interaction with the amide O of the opposite arm to orient the phenyl rings outwards from the calix unit. Thus the two tethered arms undergo an unusual crossover based on these unique interactions in the crystal structure.

Kumar *et al.* reported thiacalix[4]tube **28** (Fig. 23),<sup>43</sup> which is composed of two thiacalix[4]arene units and two diimine linkages. In the crystal structure, both thiacalix[4]arene cores adopt the same pinched cone conformation and no difference in their  $\theta$  values (Table 1). In either thiacalix[4]arene core, both OH groups are titled into the cavity and create two O–H...O H-bonds with the same ether O atom. In addition, other three H-bonds were found between the OH groups and the imine N atom, as well as two S atoms. This thiacalix[4]tube receptor can quantitatively extract Ag<sup>+</sup> ion from aqueous into organic phase under neutral conditions.

Compounds **29–33** (Fig. 24),<sup>44,45</sup> a family of thiacalix[4]arene derivatives modified at its lower and upper rims, all give a cone conformation with similar  $\theta$  ranges except for **33** (Table 1). These molecules show the same type of intramolecular O–H...O and O–H...S H-bonds as in **23** discussed above, but they

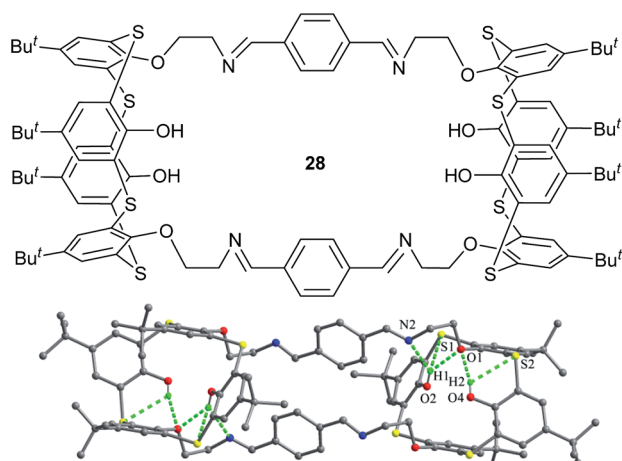


Fig. 23 Chemical and crystal structures of compound **28**, showing intramolecular H-bonds.

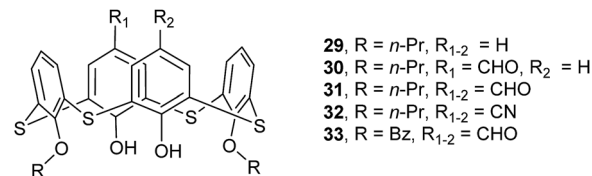


Fig. 24 Structures of compounds **29–33**.

demonstrate diverse assemblies in the solid state. Both **29** and **30** (with one CHO group) (Fig. 25a) are assembled into a kind of head-to-head dimers *via* interdigitation of aromatic rings with  $\pi$ – $\pi$  and C–H... $\pi$  contacts, while **31** (with two CHO groups) is associated into a different head-to-head dimer through  $\pi$ – $\pi$  contact and weak C6–H6...O5 and C7–H7...O5 H-bonds (Fig. 25b). This could be ascribed to the introduction of the second CHO group. In comparison, molecule **32** (with two CN groups) displays a remarkable difference in the assemblies (Fig. 25c). A unique off-set kind of dimer is formed *via* Cl...Cl and Cl... $\pi$  contacts. In such a dimer, two CHCl<sub>3</sub> molecules linked by Cl...Cl contact, serve as a bridge to join two vicinal thiacalix[4]arene molecules by Cl... $\pi$  contacts, with one Cl atom of the CHCl<sub>3</sub> molecule lodged into the  $\pi$ -basic host cavity.

Amongst these compounds, **33** gives the biggest  $\theta$  range (Table 1) owing to the replacement of *n*-propyl moiety with bigger benzoyl group. In the packing, it does not generate a head-to-head dimer but yield a tail-to-tail one by interaction between benzoyl groups with  $\pi$ – $\pi$  stacking (Fig. 25d).

In addition, they all produce a similar type of honeycomb channel architectures. For instance, six molecules of **30** are packed in a back-to-back fashion, creating a disc-like hexamer

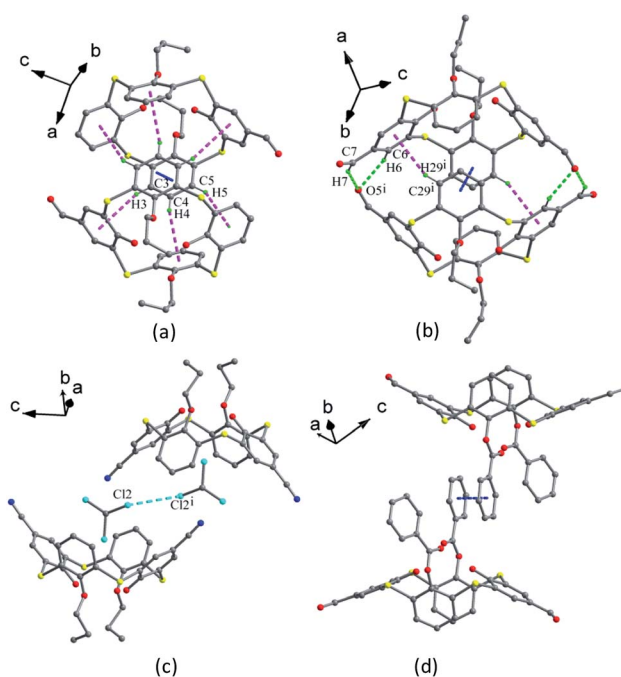


Fig. 25 Dimers of **30** (a), **31** (b), **32** (c) and **33** (d), showing diverse intermolecular interactions involving  $\pi$ – $\pi$  (blue), C–H... $\pi$  (pink), C–H...O (green) and Cl...Cl (cyan) contacts.





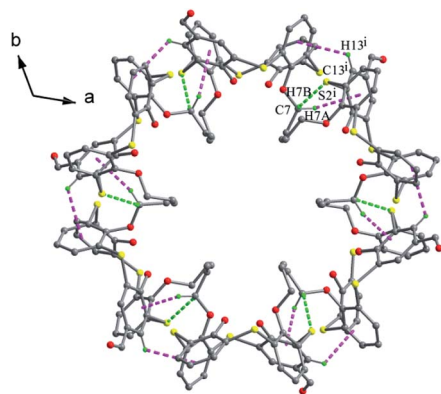


Fig. 26 A disc-like hexamer of **30**, showing intermolecular C–H...S (green) and C–H... $\pi$  (pink) interactions.

via weak C7–H7B...S2, C13–H13... $\pi$  and C7–H7A... $\pi$  contacts (Fig. 26), while a disordered CHCl<sub>3</sub> molecule locates in the centre of such a hexamer with C–H...Cl contacts. Then, these hexamers aggregate into a channel through C–H...S and S... $\pi$  interactions. And neighbouring channels connect to form a honeycomb architecture by inter-channel  $\pi$ – $\pi$  and C–H... $\pi$  contacts.

In contrast, few of 1,2-disubstituted thiacalix[4]arenes have been obtained in a cone conformation up to now, thus their crystal structures are rarely reported. An only known example is 1,2-bistriflate thiacalix[4]arene derivative **34** (ref. 46) (Fig. 27). In the crystal structure, there exist two molecules **A** and **B** in its unit cell. Both molecules adopt a pinched cone conformation and show different  $\theta$  values (Table 1). As shown in Fig. 27, such a pinched cone conformer is stabilized by an intramolecular O–H...O H-bond between the two OH groups and O...S contacts between the triflate groups and S bridges. Additionally, in the packing, intermolecular F...F and O...S contacts are generated and further fix its crystal structure.

#### 2.4 O-Tri/tetrasubstituted thiacalix[4]arenes

Thiacalix[4]arene tridiethylthiophosphate **35** (ref. 47) (Fig. 28) is a sulphur-enriched compound and can efficiently extract Ag<sup>+</sup> ion from water into dichloromethane. In the solid state, it shows a markedly distorted cone conformation with four  $\theta$  angles in great difference (Table 1). In such a conformer, the sole OH group takes part in the formation of H-bonds with O8 and S4 atoms (Fig. 29a).

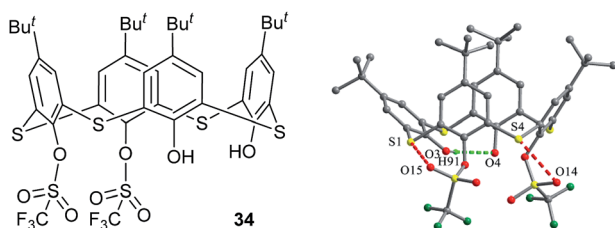


Fig. 27 Chemical and crystal structures of compound **34**, showing intramolecular H-bond and O...S contacts.

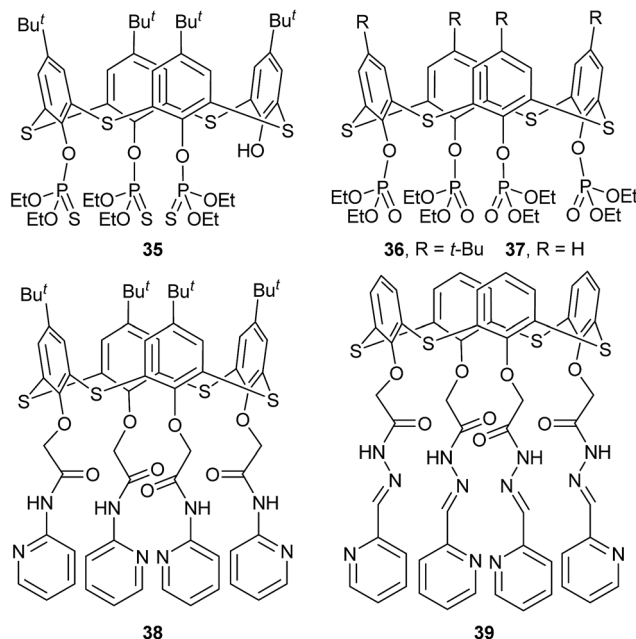


Fig. 28 Structures of compounds **35**–**39**.

Tetraphosphorylated thiacalix[4]arenes **36** and **37** (ref. 48) (Fig. 28) are good ligands that can selectively extract Pd<sup>2+</sup> ion from automotive catalyst residue solution. In the solid state, they adopt a cone conformation with  $\theta$  ranges of 78.7–123.8° and 65.2–136.7° (Table 1), respectively. Intramolecular S...O interactions between S bridges and P=O units were found to stabilize the conformers of either molecule (Fig. 29b and c). In addition, for **37**, its conformer is further governed by intramolecular C–H... $\pi$  interactions. In the packing (Fig. 30), 1-D chains of them are formed with C–H... $\pi$  interactions between aromatic rings and ethyl H atoms of vicinal molecules. In addition, their P=O groups also participate in making their three-dimensional supramolecular assemblies via H-bonds.

Thiacalix[4]arene derivative **38** (ref. 49) (Fig. 28) possesses four amide-bridged pyridine arms and takes a cone conformation with a small  $\theta$  range of 106.0–116.9° (Table 1). All amide O atoms cannot act as an acceptor to form intramolecular N–H...O H-bonds as they orient outwards the cavity due to their electron repulsion. However, all NH groups can serve as a donor to create N–H...O H-bonds with the phenolic O atom of the same arm, and generate three N–H...S H-bonds with the S bridges (Fig. 29d). The O atoms of some amide groups play an important role in the formation of intermolecular H-bonds with H<sub>2</sub>O molecules in the packing. This molecule shows high affinity towards Ag<sup>+</sup> ion in solution owing to the introduction of pyridine function.

Podyachev *et al.* reported thiacalix[4]arene derivative **39** (Fig. 28),<sup>50</sup> having four identical hydrazone-bridged pyridine arms at the lower rim. The thiacalix[4]arene core displays a cone conformation with a large  $\theta$  range of 67.5–146.5° (Table 1), where two opposite phenolic rings inclined towards the cavity, and the other two point outwards. Compared with **38**, only two NH groups can yield similar N–H...O bonds with the ether O



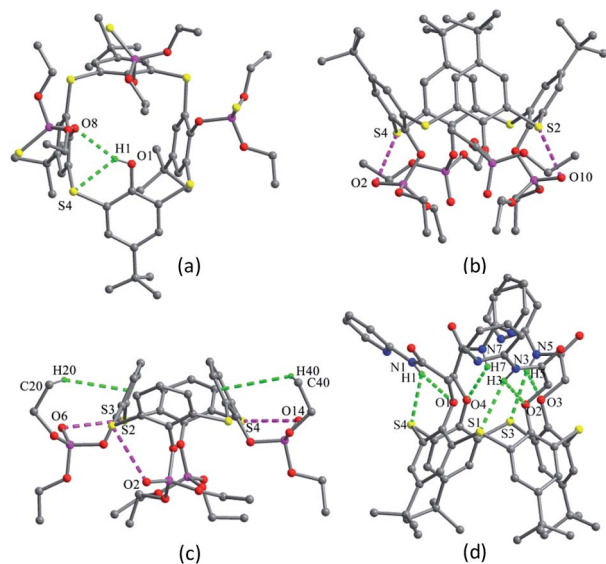


Fig. 29 Crystal structures of **35** (a), **36** (b), **37** (c), and **38** (d) showing intramolecular H-bonds.

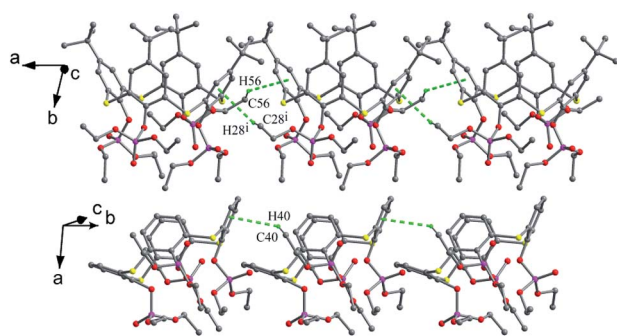


Fig. 30 1-D chains of **36** (top) and **37** (bottom) showing C–H... $\pi$  interactions.

atom of the same arm (Fig. 31). The other two NH groups can produce the intermolecular N–H...O bonds with adjacent host and guest molecules, respectively. In addition, there is an intramolecular N46–H46...O38 H-bond between two amide groups of the vicinal arms. In the packing, a centrosymmetric dimer is also built by two N30–H30...O30 H-bonds.

Doubly bridged thiacalix[4]arenes **40–42** (Fig. 32),<sup>51</sup> obtained by the aminolysis of thiacalix[4]arene tetraacetate with various

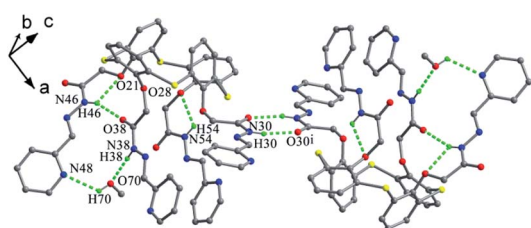


Fig. 31 Crystal structure of **39**, showing a dimer with intra- and intermolecular H-bonds.

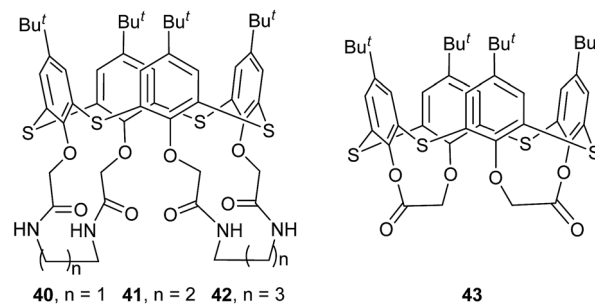


Fig. 32 Structures of compounds **40–43**.

$\alpha,\omega$ -diamines, generate cage-like structures possessing well preorganised array of –NH–CO– binding sites in the lower rim. X-ray analysis indicates that they all take a cone conformation and possess a very similar configuration with  $\theta$  ranges of 92.6–131.7°, 90.2–132.8° and 90.3–132.5° (Table 1), respectively. One pair of opposing aromatic rings points outwards the cavity, while the other pair tilts inwards. For three molecules, there is one strong intramolecular N–H...O H-bond existed between two crown moieties, resulting in one amide C=O group distorting into the cavity. Moreover, there is one intra-crown H-bond formed between two amide groups in **40** (Fig. 33a) and **41** (Fig. 33b), but between one amide group and one ether O atom in **42** (Fig. 33c). Additionally, an intramolecular N–H...S H-bond was found in the crystal structures of **40** and **42**. All these H-bonds together govern the cone conformers.

In the crystal structure of **43** (Fig. 33d),<sup>52</sup> a dilactone derivative of **1**, although the presence of two lactone bridges induces the cone conformer distorted, the whole structure still has approximate  $C_2$  symmetry with  $\theta$  values of 87.4, 140.8, 91.2 and 142.8°. So two opposing aromatic rings are almost coplanar, while the other two are tilted outwards making lactone bridges bent towards the cavity. In such a conformation, two kinds of

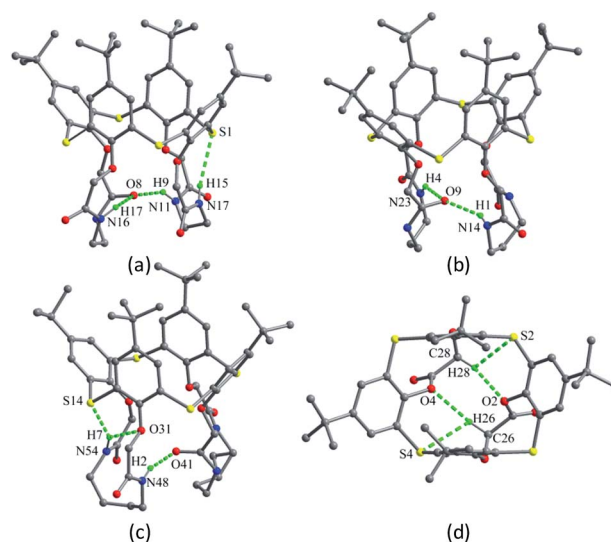


Fig. 33 Crystal structures of **40** (a), **41** (b), **42** (c) and **43** (d), showing intramolecular H-bonds.



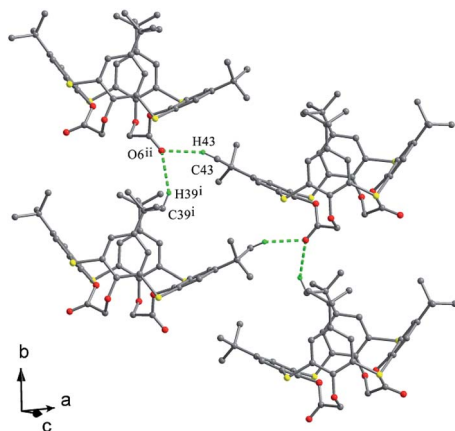


Fig. 34 Partial packing structure of 43, showing H-bonds.

intramolecular H-bonds exist between lactone methylene H28, H26 atoms and vicinal O2, O4 atoms with contribution of bridging S atoms. In the packing (Fig. 34), only carbonyl O6 participates in the soft intermolecular H-bonds with two H atoms of *t*-butyl groups from two molecules, creating an infinite network of molecules.

In the crystal structures of dibromothiactalix[4]arenes **44** and **45** (Fig. 35),<sup>53,54</sup> the thiactalix[4]arene units give different pinched cone conformations with large  $\theta$  ranges of 75.0–143.5° and 65.6–153.9° (Table 1), respectively. For **44** (Fig. 36a), two brominated benzene rings are bent outwards the cavity with a long Br...Br distance of 13.17 Å. However, the other two benzene rings, one of which is bent towards the cavity, are almost parallel to each other with a dihedral angle of 2.99°. One of the ether O atoms makes two H-bonds with both OH groups. Whereas, for **45** (Fig. 36b), two brominated aromatic rings also incline outwards the cavity with a slight longer Br...Br distance of 13.82 Å. Remarkably, the other two aromatic rings are not parallel and both tilt inwards with a large dihedral angle of 33.4°. This may be ascribed to the destruction of the two H-bonds and the influence of the bulky CH<sub>2</sub>CO<sub>2</sub>Me moieties.

In the packing of **44**, two different molecular chains, one with alternating (Fig. 37a) and the other with tail-to-tail orientations (Fig. 37b), are formed by intermolecular offset-face-to-face  $\pi$ - $\pi$  stackings of the aromatic rings. However, in the case of **45** (Fig. 37c), an infinite zigzag 1-D chain is formed by intermolecular C-H...S H-bonds and S...S contacts between the adjacent molecules. Finally, such chains are associated into bilayers by a combination of interchain C-H...O H-bonds.

Lhoták *et al.* reported that tetrasulfinyl thiactalix[4]arene **46** (Fig. 35),<sup>55</sup> synthesized by selective oxidation of tetramethoxy

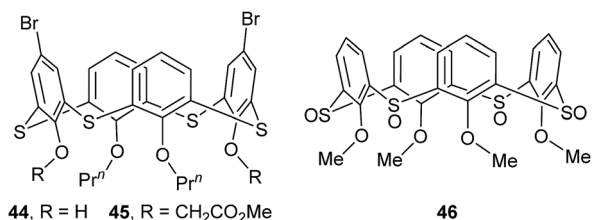


Fig. 35 Structures of compounds 44–46.

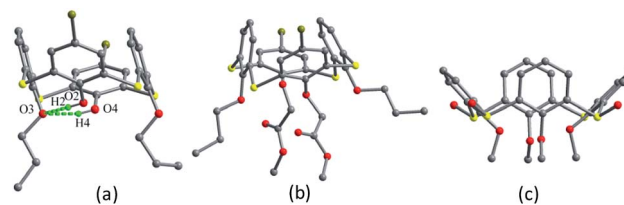


Fig. 36 Crystal structures of 44 (a), 45 (b) and 46 (c).

thiactalix[4]arene, adopts a nearly  $C_2$  symmetric cone conformation with  $\theta$  values of 106.7, 134.9, 110.9 and 132.0°. Such structure is influenced by intermolecular C35–H35... $\pi$  contacts between the OMe group and its linked aromatic ring of vicinal molecules (Fig. 38). Therefore, an infinite chain is produced and the OMe unit of one molecule is immersed in the cavity of the other one in the packing.

Briefly, only few of thiactalix[4]arenes show a perfect cone conformation possessing the same  $\theta$  values, while the majority of them give a pinched or distorted cone conformation having different angles. In general, thiactalix[4]arene molecules with four OH or/and NH<sub>2</sub> groups at the lower rim exhibit  $C_4$  or near  $C_2$ -symmetry and form an intramolecular annular H-bonding array. For most *O*-mono- and di-substituted thiactalix[4]arenes, they are favored to take a pinched cone conformation as their free OH groups create asymmetrically intramolecular H-bonds in a sequential pattern from one OH group to the ether O atom or in such a way that one ether O atom forms two H-bonds with its vicinal OH groups. However, for *O*-tetrasubstituted thiactalix[4]arenes, they usually exhibit different cone conformers as their substitutes are changed. In the assemble, versatile interactions involving H-bonds, C-H... $\pi$ ,  $\pi$ - $\pi$  and hetero atom contacts play a key role in constructing the supramolecular assemblies and fixing the conformations.

### 3. 1,3-Alternate structures of thiactalix [4]arenes

Thiactalix[4]arenes with various functional groups are very popular because of their highly binding affinity. Especially,

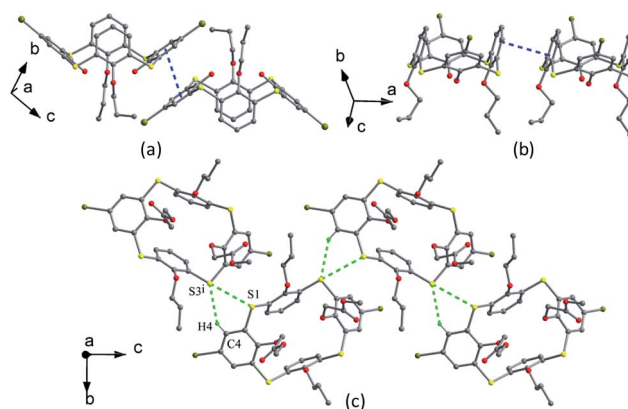


Fig. 37 Partial packing structures of **44** in alternating orientations between the phenolic rings (a) and in tail-to-tail orientations between the ether-substituted rings (b), and a 1-D zigzag chain of **45** (c).



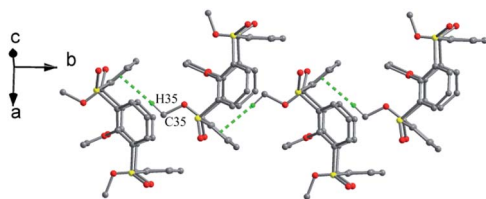


Fig. 38 A 1-D chain of **46** with C–H... $\pi$  interactions.

these groups in 1,3-alternate orientations markedly enhance their binding properties. Thiacalix[4]arene derivatives are in a 1,3-alternate conformation rather than a cone one based on the chemical modification conditions and the substituents attached. The most such compounds are homo- or hetero-tetrasubstituted thiacalix[4]arene derivatives at the lower rim, and some S-oxidized derivatives.

### 3.1 S-Oxydic thiacalix[4]arenes

The conformation of some thiacalix[4]arenes may be changed upon oxidation of their S bridges. Tetrasulfinyl thiacalix[4]arenes **47** and **48** (Fig. 39) could be obtained *via* selective oxidation of the four S bridges.<sup>56,57</sup> In the solid state, both compounds display a similar 1,3-alternate conformation with a narrow  $\theta$  range of 79.5–94.8° and the same  $\theta$  value of 73.5° (Table 2), respectively. All O atoms of their S=O units are alternately oriented above and below the *R* plane. This kind of conformers is governed by four alternate O–H...O H-bonds between the OH groups and the S=O units, with average bond distances of 2.67 Å for **47** (Fig. 40a) and 2.65 Å for **48** (Fig. 40b). Interestingly, a 3-D network is formed by intermolecular  $\pi$ – $\pi$  stacking between all four aromatic rings of **48** (Fig. 41). However, such a network was not observed in the crystal structure of **47**, owing to the presence of bulky *t*-butyl groups.

Using the similar strategy, the corresponding tetrasulfonyl derivative **49** (ref. 58) (Fig. 39) could be prepared and shows a typical 1,3-alternate conformation with the same  $\theta$  value of 89.5°. Dissimilar to **47** and **48**, all sulfonyl O atoms of **49** point outwards the cavity. This conformer can be rationalized by the formation of H-bonds between the OH groups and the SO<sub>2</sub> units (Fig. 40c). In the packing, a 3-D network is built by intermolecular H-bonds between the OH and SO<sub>2</sub> moieties belonging to adjacent molecules (Fig. 42).

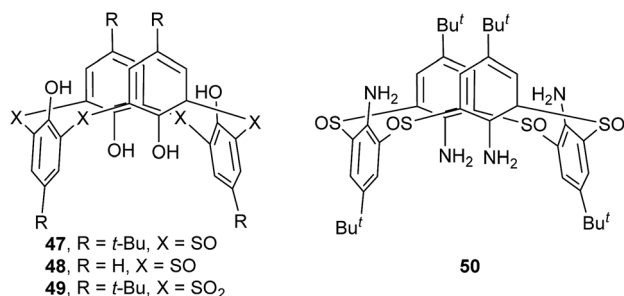


Fig. 39 Structures of compounds **47**–**50**.

Table 2 The  $\theta$  angles of compounds **47**–**93**<sup>a</sup>

Compd.	$\theta$ (°)			
<b>47</b>	79.5	86.6	94.8	87.6
<b>48</b>	73.5	73.5	73.5	73.5
<b>49</b>	89.5	89.5	89.5	89.5
<b>50</b>	95.5	95.5	95.5	95.5
<b>51</b>	107.1	105.4	107.1	105.4
<b>52</b>	102.1	106.6	102.1	106.6
<b>53</b>	93.6	94.9	93.6	94.9
<b>54</b>	110.1	113.1	122.9	116.9
<b>55</b>	108.3	117.8	124.7	110.1
<b>56<sup>b</sup></b>	92.2	97.7	98.7	93.9
<b>57</b>	101.9	107.4	118.4	110.1
<b>58</b>	98.2	110.9	112.9	109.6
<b>59</b>	116.1	117.8	116.1	117.8
<b>60</b>	109.2	112.9	125.7	115.5
<b>61</b>	111.6	115.3	112.1	115.0
<b>62</b>	91.2	92.2	91.2	92.2
<b>63</b>	103.9	104.6	103.9	104.6
<b>64</b>	83.5	88.8	86.4	87.8
<b>65</b>	97.1	103.0	98.3	114.7
<b>66</b>	100.3	102.4	103.9	102.6
<b>67</b>	104.3	112.5	121.6	107.9
<b>68</b>	104.2	116.5	104.2	116.5
<b>69</b>	102.4	116.8	108.4	115.2
<b>70</b>	109.2	112.9	110.6	119.5
<b>71</b>	86.3	88.2	86.3	88.2
<b>72</b>	106.0	113.8	118.4	108.3
<b>73</b>	92.5	103.5	107.4	100.8
<b>74A</b>	108.1	121.1	121.6	118.1
<b>74B</b>	113.9	119.1	118.0	120.0
<b>75</b>	109.8	112.4	122.0	118.2
<b>76</b>	110.7	113.3	125.4	113.5
<b>77</b>	100.9	102.9	100.9	102.9
<b>78</b>	107.2	108.6	107.2	108.6
<b>80</b>	103.7	107.5	103.7	107.5
<b>81</b>	103.1	107.2	123.0	113.6
<b>82</b>	101.5	112.1	107.6	111.4
<b>83</b>	89.5	95.8	101.9	102.8
<b>84</b>	103.1	110.5	107.3	105.9
<b>85</b>	103.9	107.2	111.4	104.8
<b>86</b>	101.0	106.7	110.6	117.9
<b>87</b>	102.1	106.1	108.4	113.8
<b>88</b>	101.4	102.2	112.6	104.9
<b>89</b>	106.4	111.5	107.4	114.2
<b>90A</b>	109.2	116.3	116.9	111.8
<b>90B</b>	111.3	114.4	114.9	114.7
<b>91</b>	103.6	118.7	117.9	111.4
<b>92A</b>	66.1	147.7	74.2	154.6
<b>92B</b>	72.8	141.8	73.7	155.9
<b>93</b>	111.4	114.0	115.9	114.3

<sup>a</sup> Data obtained by calculation with Diamond Version 3.0. <sup>b</sup> Data obtained from refs.

Tetrasulfinyl thiacalix[4]arene analogue **50** (ref. 27) (Fig. 39) also gives a typical 1,3-alternate conformation with the same  $\theta$  value of 95.5°. Four intramolecular N–H...O H-bonds are yielded between the NH<sub>2</sub> groups and the sulfinyl O atoms (Fig. 40d). Moreover, a 2-D network is made by intermolecular H-bonds produced in the same way (Fig. 43). It should note that although **48**, **49** and **50** all possess four identical  $\theta$  angles, they increase in order, which may be attributed to the influence of *de-t*-butyl and the kinds of H-bonds.



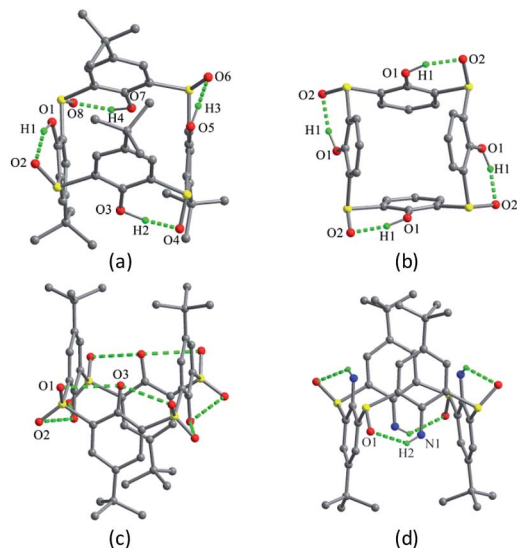


Fig. 40 Crystal structures of 47 (a), 48 (b), 49 (c) and 50 (d), showing intramolecular H-bonds. All protons of the OH groups were not found in the crystal of 49.

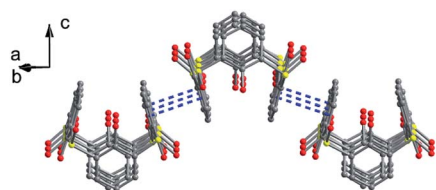


Fig. 41 A 3-D network of 48 through stacking of the aromatic groups.

Thiacalix[4]arene **51** (Fig. 44),<sup>59</sup> a derivative of **49** with four ether chains ended with Cl atom, also takes a 1,3-alternate conformation and all sulfonyl O atoms point outwards the cavity. In the solid state, although no hard H-bonds are found owing to the etherification of all OH groups, various soft H-bonds involving intra- and intermolecular C–H...O govern the conformation. Interestingly, an unusual 24-membered ring is created by a similar H-bonding array consisting of C–H...O H-bonds rather than O–H...O H-bonds in **49**. In this macrocycle, both O atoms of each sulfonyl unit act as H-bond acceptor to H atoms of the two vicinal methylene groups closer phenolic rings. Thus it gives two pairing  $\theta$  values of 107.1 and 105.4°, larger than that found in **49**. In the packing, an infinite zigzag 1-D chain is formed by four intermolecular C–H...O H-bonds (Fig. 45).

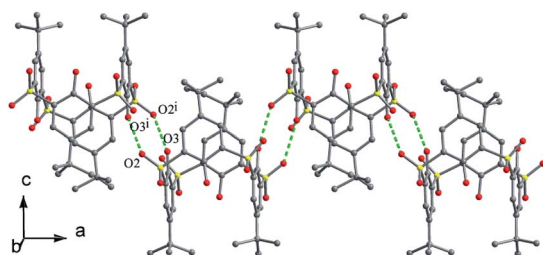


Fig. 42 A 1-D chain of 49 with intermolecular H-bonds.

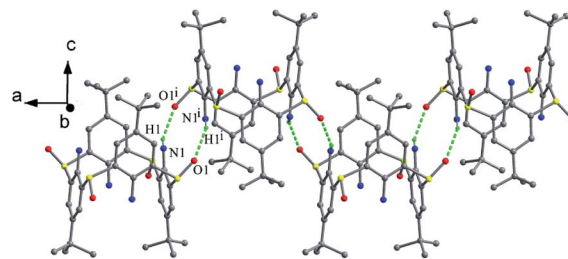


Fig. 43 A 2-D network of **50** built by intermolecular N–H...O H-bonds.

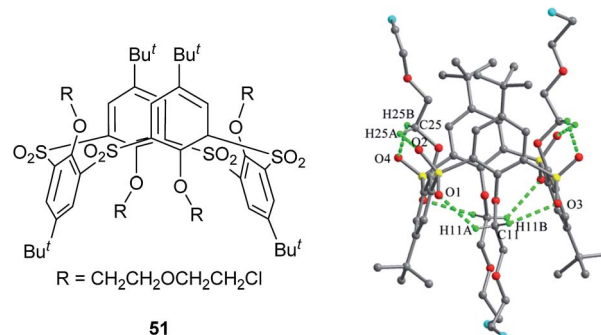


Fig. 44 Chemical and crystal structures of compound **51** with intramolecular H-bonding array.

### 3.2 O-Homosubstituted thiacalix[4]arenes

O-Homosubstituted thiacalix[4]arenes can be readily made *via* incorporating four identical substituents at the lower rim under the controlled reaction conditions.<sup>6–9</sup> Compounds **52** and **53** (Fig. 46),<sup>60</sup> methyl ether derivatives of thiacalix[4]arenes, show different conformational behaviour in the solid state. Molecule **52** adopts a 1,3-alternate conformer with two pairs of  $\theta$  angles (Table 2) upon crystallization from CH<sub>2</sub>Cl<sub>2</sub> solvent (Fig. 47a). Square box-shaped cavities of thiacalix[4]arenes are packed parallel to each other and create infinite channels (Fig. 48), of which the inner and outer are filled with H<sub>2</sub>O and CH<sub>2</sub>Cl<sub>2</sub> molecules, respectively. Whereas, **52** can also take a 1,2-alternate conformation with two pairing  $\theta$  angles of 96.3 and 112.5°

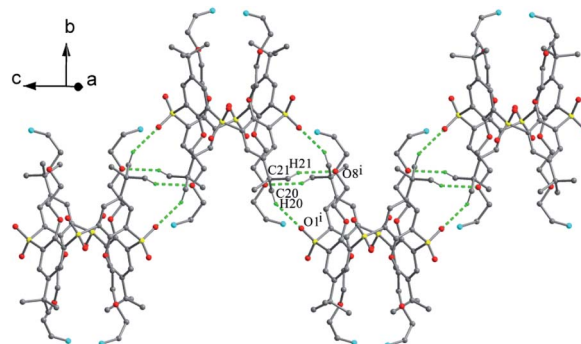


Fig. 45 A 1-D chain of **51** formed by intermolecular C–H...O H-bonds.



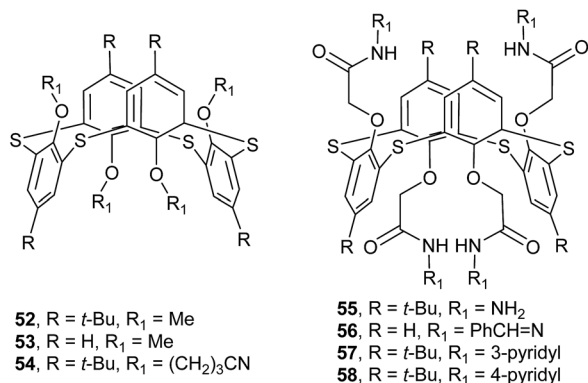


Fig. 46 Structures of compounds 52–58.

when crystallization from bulky solvents such as Me<sub>2</sub>CHOH or *p*-xylene as they cannot accommodate within the channels (Fig. 47b). However, upon crystallization from different solvents, molecule 53 gives a mixture of cone and 1,3-alternate conformers (3 : 1) rather than a single one (Fig. 47c). This difference can be ascribed to the loss of *t*-butyl groups. In the packing (Fig. 48), an infinite channel is constructed with regularly alternating cone and 1,3-alternate conformers *via* a combination of C–H···π and π–π contacts. It should be noted that the methoxy groups are too small to block the conformational interconversion because of the absence of any H-bonds and efficient sterical hindrance.

Molecule 54 (Fig. 46),<sup>61</sup> a thiacalix[4]arene derivative functionalized with four cyanopropyl groups, adopts a 1,3-alternate conformation with four  $\theta$  angles ranging from 110.1 to 122.9° (Table 2). An intramolecular C–H···N H-bond is yielded between CN and OCH<sub>2</sub> units in the same arm (Fig. 49a). In the packing, a 2-D network is produced by the combination of intermolecular C–H···N and C–H···S H-bonds between vicinal molecules (Fig. 50). In addition, the CHCl<sub>3</sub> molecules are packed in the crystal by C–H···N H-bonds.

Thiacalix[4]arene 55 (Fig. 46),<sup>62</sup> bearing four hydrazide arms, gives a 1,3-alternate conformation with four  $\theta$  values from 108.3 to 124.7° (Table 2). One of the hydrazide arms on each side directs into the cavity and creates an intramolecular N–H···O H-bond with the adjacent ether O atom (Fig. 49b). Thus, the H<sub>2</sub>O molecule locates outside the cavity. In the packing, a centrosymmetric dimer is produced by cooperative N45–H45···O30 H-

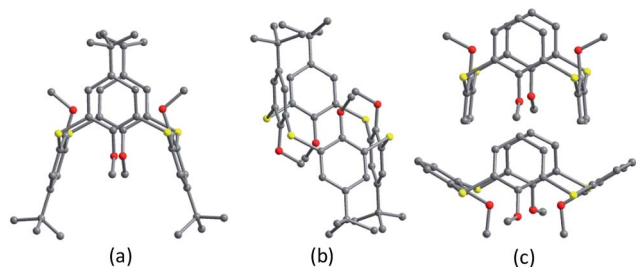
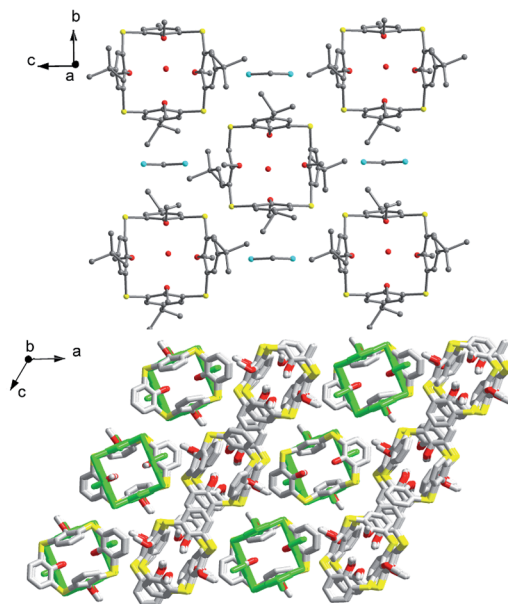


Fig. 47 Crystal structures of 52 (a) in 1,3-alternate, (b) in 1,2-alternate, and 53 (c) in cone and 1,3-alternate.

Fig. 48 Partial packing structures of 52 (top) with CH<sub>2</sub>Cl<sub>2</sub> and H<sub>2</sub>O, and 53 (bottom) with cone and 1,3-alternate (green) conformers (3 : 1).

bonds (Fig. 51). Then such dimers associate into molecular layers with H<sub>2</sub>O bridges linked by O–H···O H-bonds.

Compound 56 (Fig. 46),<sup>50</sup> a derivative by replacing four pyridyl units of 39 (Fig. 28) with phenyl groups, adopts a 1,3-alternate conformation with four similar  $\theta$  values (Table 2) rather than a pinched cone conformation in 39. Although both compounds could interchange their conformations owing to removal of *t*-butyl groups, only 39 keeps a pinched cone conformer due to the hindrance of intermolecular N–H···O and O–H···N H-bonds between two vicinal arms with a MeOH-

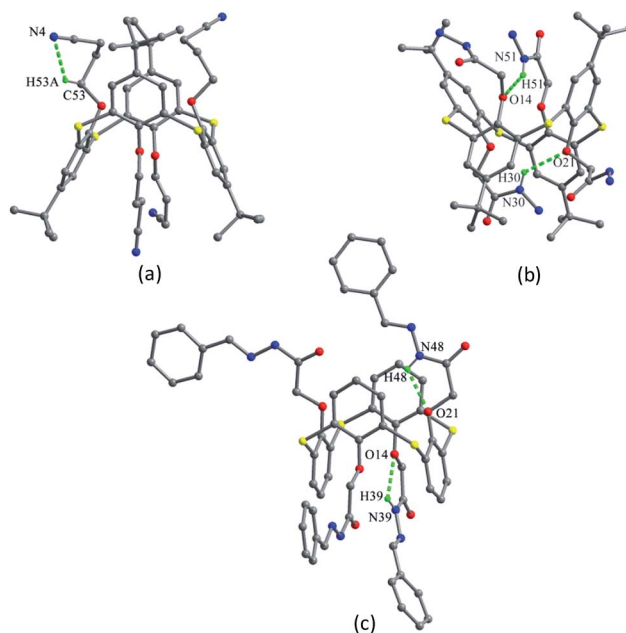


Fig. 49 Crystal structures of 54 (a), 55 (b) and 56 (c) showing intramolecular H-bonds.



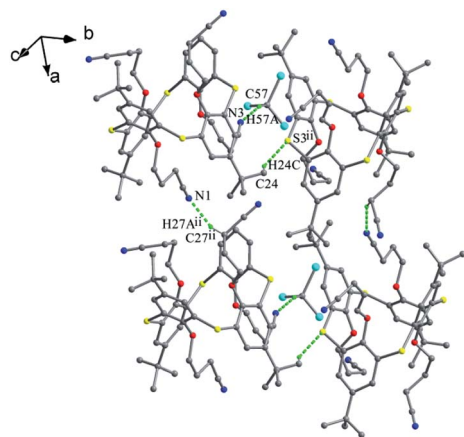


Fig. 50 Partial packing structure of **54**, showing intermolecular H-bonds.

bridge. For **56** (Fig. 49c), only two intramolecular N-H $\cdots$ O H-bonds are formed in the same arm. In the packing (Fig. 52), an infinite molecular chain is produced by intermolecular N58–H58 $\cdots$ O48 H-bonds between the NH and C=O groups. These chains are associated in parallel way into a 3-D network bridged by H<sub>2</sub>O molecules, where four vicinal thiacalix[4]arene molecules are interlinked *via* hard H-bonds involving two NH and two C=O groups, as well as a pair of H<sub>2</sub>O molecules.

In some 1,3-alternate thiacalix[4]arenes bearing heterocyclic rings, the hetero atoms can play an additional acceptor to yield H-bonds and complex metal ions. Thiacalix[4]arenes **57** and **58** (Fig. 46),<sup>63</sup> anchoring isomeric pyridine rings by amide linkage, display a 1,3-alternate conformation. Both molecules can bind Ag<sup>+</sup> ion selectively in solution, while the binding efficiency is influenced by the structures of aminopyridyl pendent arms, the former shows a better extraction capacity. In the solid state, it was found that they give the similar thiacalix[4]arene shape with four  $\theta$  values from 101.9 to 118.4, and 98.2 to 112.9° (Table 2), respectively. However, their whole molecular structures are much more asymmetrical because of the spatial different outspread of the flexible side chains. And the most significant

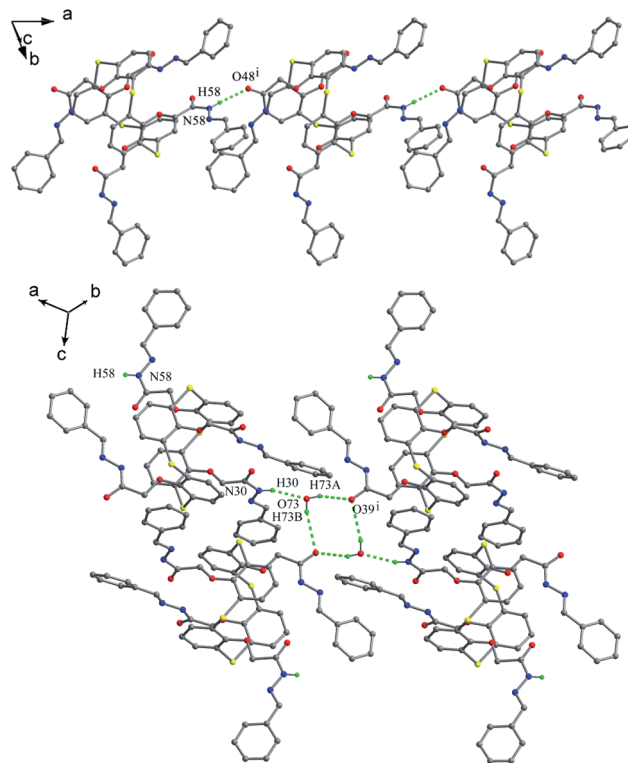


Fig. 52 Partial packing structure of **56**, showing an infinite molecular chain (top), and a tetramer linked with two water molecules (bottom).

difference between them is the orientation of aminopyridyl side chains, ascribed to the differing position of pyridyl moiety connecting to the NH moiety.

For **57** (Fig. 53), it's favored to form intramolecular hard H-bonds between the N atoms of *m*-pyridyl rings and the facing NH units of amide groups, while no such hard intermolecular H-bonds were found between the vicinal molecules as all the amide NH groups bury in the cavity of thiacalix[4]arene. Only intermolecular C–H $\cdots$  $\pi$  and C–H $\cdots$ O contacts were observed, creating a 1-D chain in a side-by-side mode (Fig. 54). Then a double stranded chain is yielded by inter-chain C62–H62 $\cdots$ O6 H-bonds between OCH<sub>2</sub> units of one strand and carbonyl O atoms of the other strand. Eventually, these double stranded chains are linked by MeOH solvent molecules in the crystal lattice.

In comparison, there is no corresponding intramolecular H-bond existed in **58** because of the pyridyl N atom at the *p*-position rather than the *m*-position, orienting outwards the cavity (Fig. 53). As a result, the amide N atoms are available for contacts with the pyridyl N atoms of adjacent molecules. As shown in Fig. 55, individual molecules of **58** are in a side-by-side orientation, yielding a 1-D chain by intermolecular N7–H7 $\cdots$ N4 H-bonds. With the help of H<sub>2</sub>O molecules, two strips of the resulting 1-D chains are further augmented to a water-bridged double strand.

Thiacalix[4]bis-crown analogue **59** (ref. 64) (Fig. 56) takes a 1,3-alternate conformation with four quite similar  $\theta$  angles (Table 2) and shows two fold rotation symmetry with an cage-like cavity. All four N–H bonds of both amide bridges are

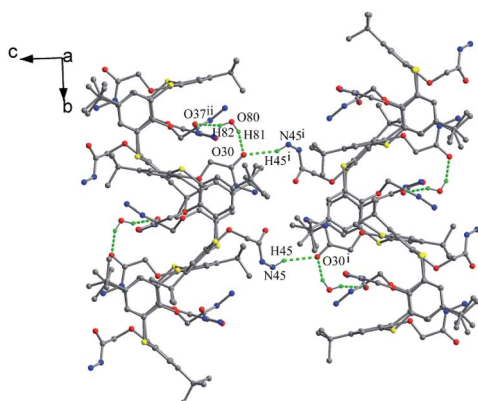


Fig. 51 Partial packing structure of **55**, showing a centrosymmetric dimer and molecular layers.



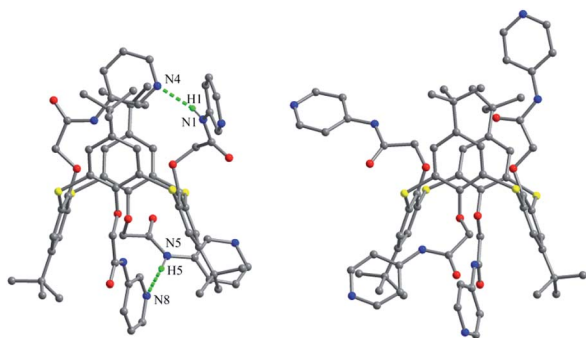


Fig. 53 Crystal structures of **57** (left) and **58** (right).

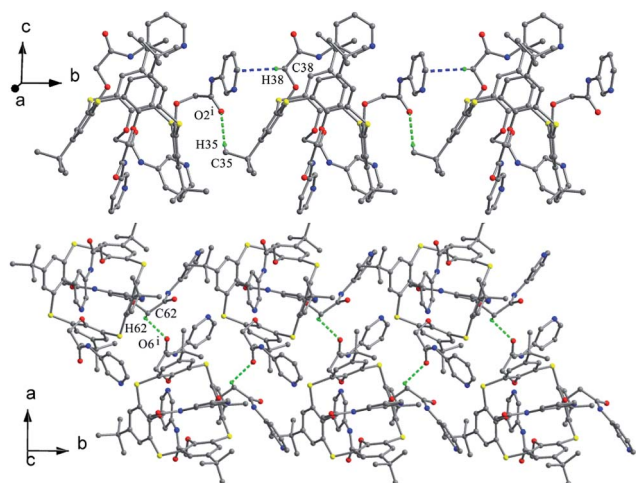


Fig. 54 Partial packing structures of **57** showing a 1-D chain (top), and a double stranded chain (bottom).

oriented into the calix cavity and generate intramolecular H-bonds to all ether O atoms.

Thiacalix[4]arenes **60** and **61** (Fig. 57),<sup>65</sup> with four thiadiazole termini, both give a 1,3-alternate conformation with similar  $\theta$

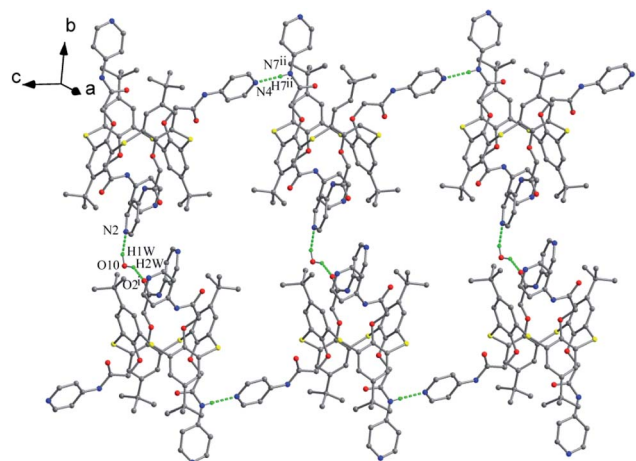


Fig. 55 Partial packing structure of **58**, showing water-bridged double strand.

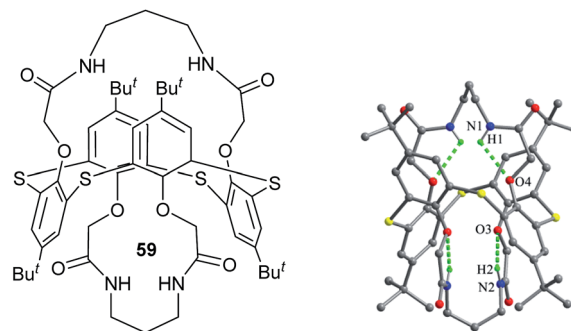


Fig. 56 Chemical and crystal structures of compound **59**, showing H-bonds.

angles (Table 2). In the solid state, a couple of opposite thiadiazole rings is nearly parallel to each other, while the other couple is perpendicular mutually (Fig. 58), forming dihedral angles of 10.9, 77.3° for **60** and 25.0, 82.0° for **61**. In the packing, molecule **60** creates a 1-D chain by weak C50–H50...N4 and C60–H60...N5 interactions between two thiadiazole rings of adjacent molecules (Fig. 59). These chains are further extended into a 2-D network by inter-chain S...S contacts between S atoms in the thiadiazole rings and 2-positional mercapto S atoms. Eventually, the 2-D networks are assembled into a 3-D supramolecular structure with the lattice water dimers through O–H...S H-bonds. In the packing of **61** (Fig. 59), two molecules are connected into a dimer by two intermolecular C–H...S contacts between the methylene H atom and the S atom in the thiacalix[4]arene unit. These dimers are further linked into a 1-D chain by S...S contacts between the same S atoms linked to the thiadiazole rings of vicinal molecules. Afterwards, these 1-D chains are assembled into a 2-D network with the methanol dimers *via* C–H...N and C–H...O H-bonds.

Compound **62** (Fig. 57),<sup>66</sup> possessing four polyether arms ended with the 4-NO<sub>2</sub>C<sub>6</sub>H<sub>4</sub> unit, crystallizes in a typical 1,3-

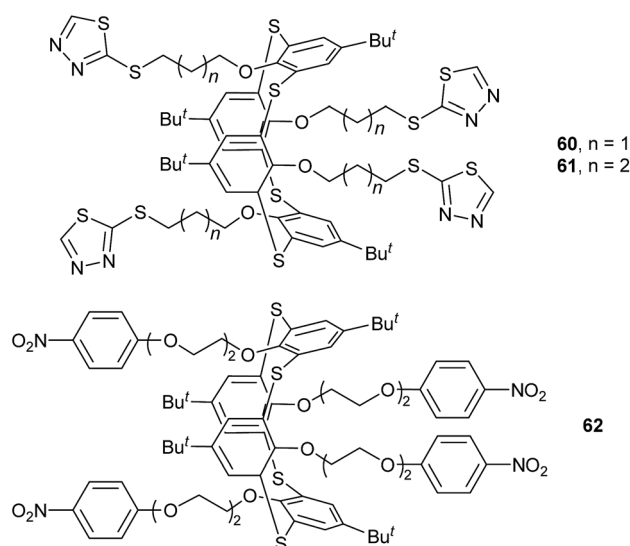


Fig. 57 Structures of compounds **60**–**62**.





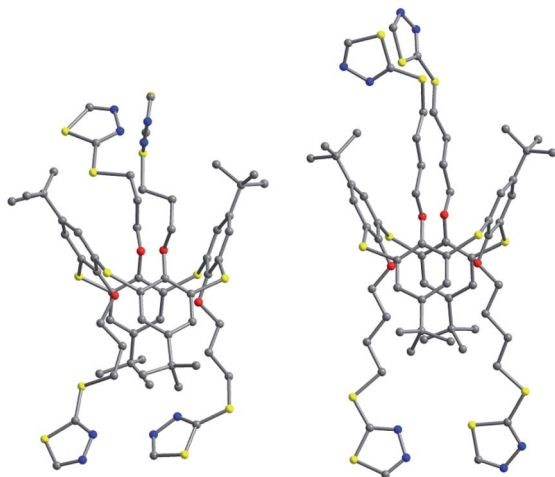


Fig. 58 Crystal structures of 60 (left) and 61 (right).

alternate conformation with two pairing  $\theta$  angles of 91.2 and 92.2°, where the four polyether arms are distorted outboard of the cavity. The terminal benzene rings are nearly parallel to the *R* plane, with interplanar angles of 14.09 and 9.05. In the packing, a 2-D array composed of the rare cyclic thiacalix[4]arene tetramers with an eighty-membered ring motif (Fig. 60) is formed by a combination of intermolecular C–H...O H-bonds. These arrays are further linked into a complex 3-D framework through interlayer C–H...S H-bonds and aromatic  $\pi$ – $\pi$  interactions.

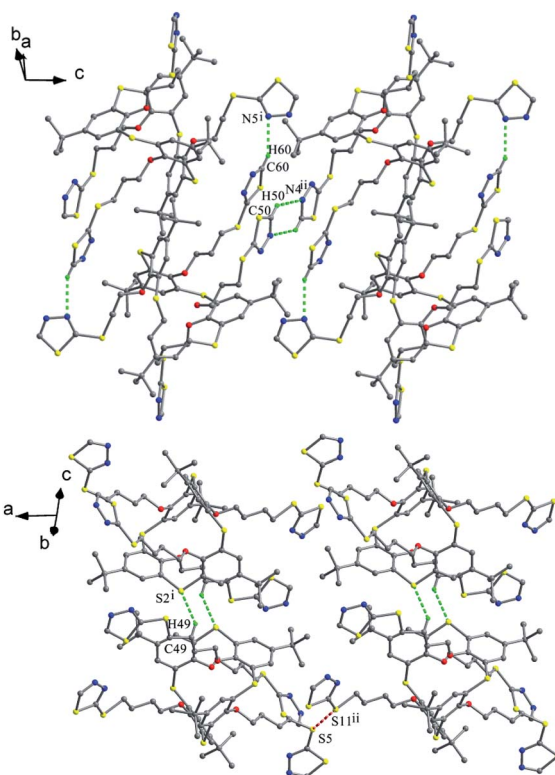


Fig. 59 Partial packing structures of 60 (top) and 61 (bottom), both showing a 1-D chain.

### 3.3 O-Heterosubstituted thiacalix[4]arenes

O-Heterosubstituted thiacalix[4]arenes are usually obtained by appending four different substituents at the lower rim *via* multiple steps. Compounds 63 and 64 (Fig. 61),<sup>67</sup> synthesized by selective hydrolysis of tetraester thiacalix[4]arene derivatives, possess both CO<sub>2</sub>H and CO<sub>2</sub>Et groups and take a 1,3-alternate conformation with two pairing  $\theta$  angles of 103.9 and 104.6°, and four similar ones from 83.5 to 88.8°, respectively (Table 2). In the crystal structure of 63 (Fig. 62), one molecule H<sub>2</sub>O lies in the calix cavity and forms two H-bonds with two CO<sub>2</sub>H groups. In the packing, a zigzag chain of 63 is apparent by intermolecular O–H...O H-bonds, locally creating a four-membered ring motif between the carboxyl OH groups (Fig. 63). However, for 64, a dimeric structure is generated *via* four intermolecular O–H...O H-bonds between CO<sub>2</sub>H groups, locally yielding two eight-membered ring motifs (Fig. 63).

Thiacalix[4]arene derivative 65 (ref. 68) (Fig. 61) contains both amide and ester groups. It has a 1,3-alternate conformation with four  $\theta$  angles from 97.1 to 114.7° (Table 2). In the solid state, it is clear that the orientations of the carbonyl O atoms of esters are outwardly orientated with respect to the cavity because of the electronic repulsion between O atoms. Interestingly, two intramolecular N–H...O H-bonds are formed (Fig. 64a): one is intra-arm type between the NH and ethereal O atom, and the other is inter-arm one between the NH and amide O atom. In solution, 65 can bind K<sup>+</sup> ion, while its structural symmetry has not been changed after complexation.

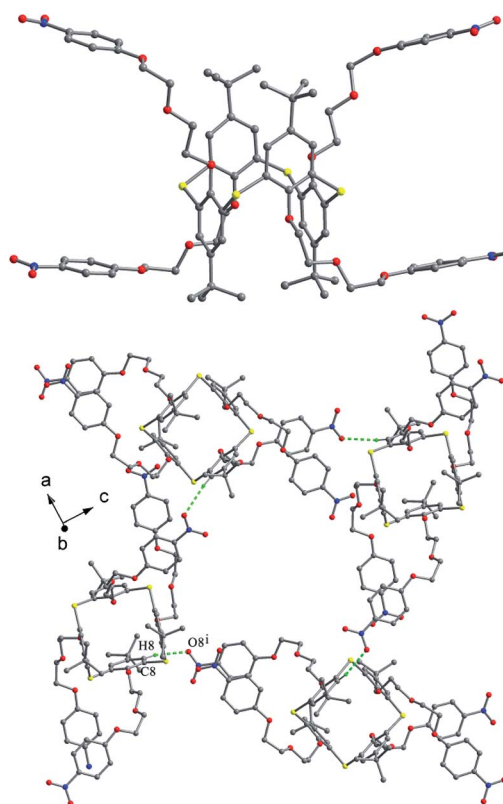


Fig. 60 Crystal structure of 62 (top) and its tetramer (bottom).



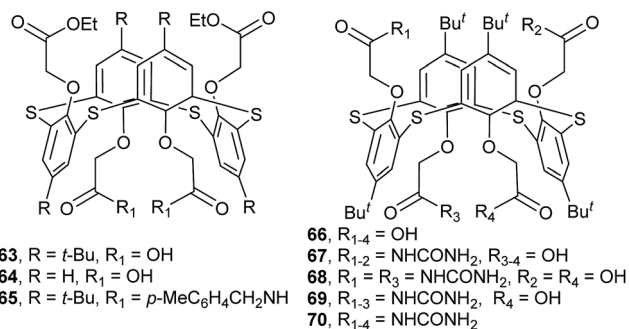


Fig. 61 Structures of compounds 63–70.

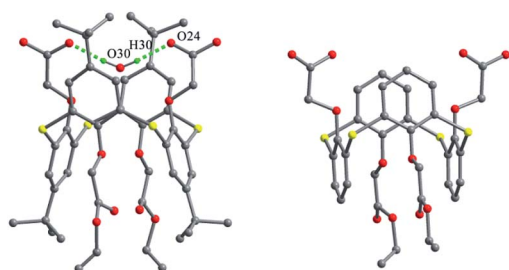


Fig. 62 Crystal structures of 63 (left) and 64 (right).

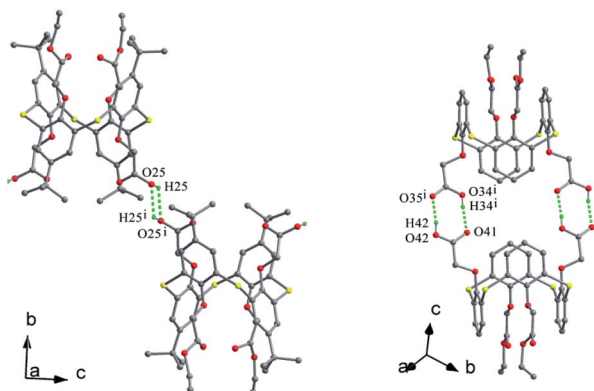


Fig. 63 Partial packing structures of 63 (left) and 64 (right), showing different H-bonded ring motifs.

Thiocalix[4]arene derivatives **66–70** (Fig. 61),<sup>15</sup> functionalized with CO<sub>2</sub>H and/or CONHCONH<sub>2</sub> groups, are all in a 1,3-alternate conformation with four similar  $\theta$  values except for **68** with two pairing  $\theta$  angles of 104.2 and 116.5° (Table 2). For **66** (Fig. 64b), there is no intramolecular H-bond between the two opposing arms, but two H<sub>2</sub>O molecules occupy the cavities made by two pairs of facing aromatic rings and create intermolecular H-bonds with the CO<sub>2</sub>H groups. For the other molecules, there are various intra- and inter-arm hard H-bonds owing to the presence of urea units. In the structures of **68** (Fig. 64c) and **70** (Fig. 64d), for instance, each urea group yields two different intra-arm N–H···O H-bonds with O atoms of CH<sub>2</sub>CO and ether moieties, respectively. Moreover, there are inter-arm O–H···O and N–H···O H-bonds between two opposing

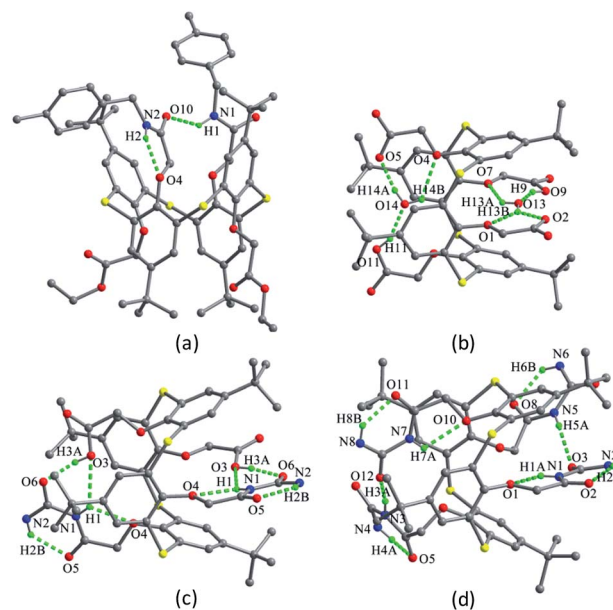


Fig. 64 Crystal structures of 65 (a), 66 (b), 68 (c) and 70 (d), showing the intra- and inter-arm H-bonds.

arms. For these molecules, the main difference is the spatial orientations of their arms. When two urea arms locate on the same side, they direct outwards due to the steric repulsion, while there are one urea arm and one CO<sub>2</sub>H group on the same side, they orientate inwards because of their inter-arm H-bonds.

In the packing of these compounds, the types of H-bonds between vicinal arms play an important role in the assemblies. For instance, two molecules of **67** create a dimer by N4–H4A···O3 and N4–H4B···O8 H-bonds. These dimers are interlinked to produce a 1-D double-stranded linear chain by the combination of N3–H3···O12 and O11–H11···O9 H-bonds (Fig. 65). While in the case of **68**, a 1-D single-stranded linear chain is formed *via* N2–H2···O2 H-bonds (Fig. 65). Moreover, self-assembly also depends on the spatial orientation of pendant arms. Through the cavity stacking fashion, only **66** can give nanotubes, in which the four pendant arms orient along the basic axis of the molecule. For the others, the inwardly orientated pendant arms obstruct the channel formation owing to protruding into the calix cavity.

Thiocalix[4]arenes **71** and **72** (Fig. 66),<sup>69</sup> modified with thio-urea or urea groups, both adopt a 1,3-alternate conformation but have different symmetry. Molecule **71** shows crystallographic C<sub>2</sub>-symmetry with two pairing  $\theta$  angles of 86.3 and 88.2°. Two pairs of facing phenolic rings exhibit approximately parallel orientations, forming interplanar angles of 3.7 and 7.4°. However, molecule **72** is asymmetrical with four different  $\theta$  angles (Table 2). Two couples of opposite phenolic rings are not parallel, creating interplanar angles of 42.1° and 44.7°. In **71** (Fig. 67a), two thiourea groups are far away from each other since two *t*-butyl groups fill in the space between them, while two urea units of **72** locate closely in a parallel way and thus create an intramolecular H-bond between them as two *t*-butyl groups are apart away (Fig. 67b). These differences may be attributed to the varied fashions of *N,N'*-disubstituted thiourea



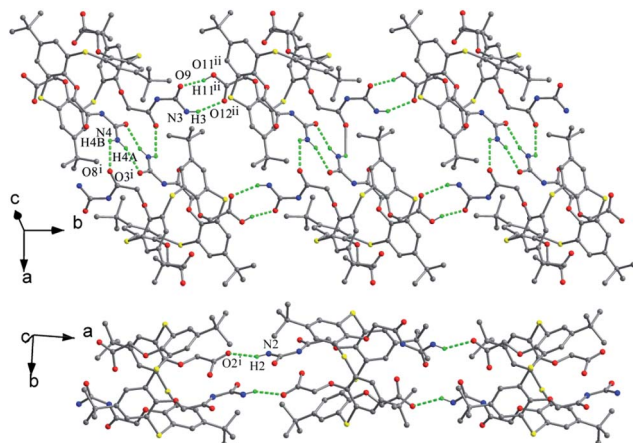


Fig. 65 Partial packing structures of **67** (top) showing a 1-D double-stranded chain and **68** (bottom) displaying a 1-D single-stranded chain.

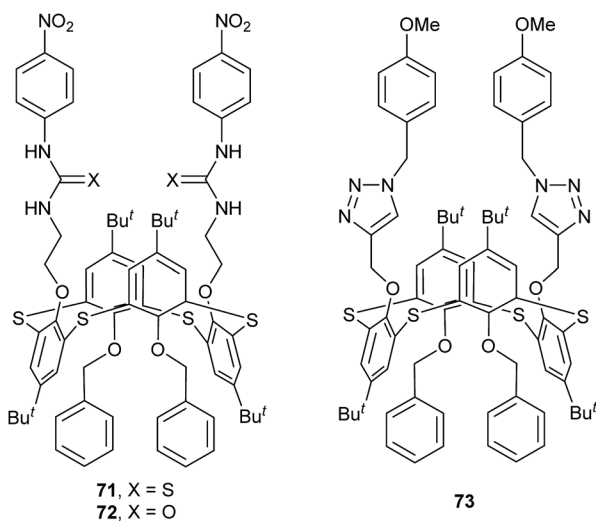


Fig. 66 Structures of compounds **71**–**73**.

(*E,Z*) and urea (*Z,Z*), which distort the macrocycle in different manners, thus yielding diverse spatial orientations of these groups. The other important factor is that the thiourea S atoms have lower H-bond accepting ability than the urea O atoms. In solution, both compounds could be used as potential receptors for anion recognition, but show poor selectivity.

Thiocalix[4]arene **73** (Fig. 66),<sup>70</sup> appending two 1,2,3-triazole bridged arms, takes a 1,3-alternate conformation with four  $\theta$  values from 92.5 to 107.4° (Table 2) (Fig. 67c). In addition, two 1,2,3-triazole rings are nearly parallel to each other with a dihedral angle of 3.0°. In the packing, a 1-D chain is produced by C–H...N H-bonds between two 1,2,3-triazole rings of adjacent molecules (Fig. 68).

Thiocalix[4]crown derivatives **74** (ref. 71) and **75** (ref. 72) (Fig. 69) both show a 1,3-alternate conformation with four similar  $\theta$  angles (Table 2). In the unit cell of **74** (Fig. 70), there are two thiocalix[4]arene molecules **A** and **B**, in which it was

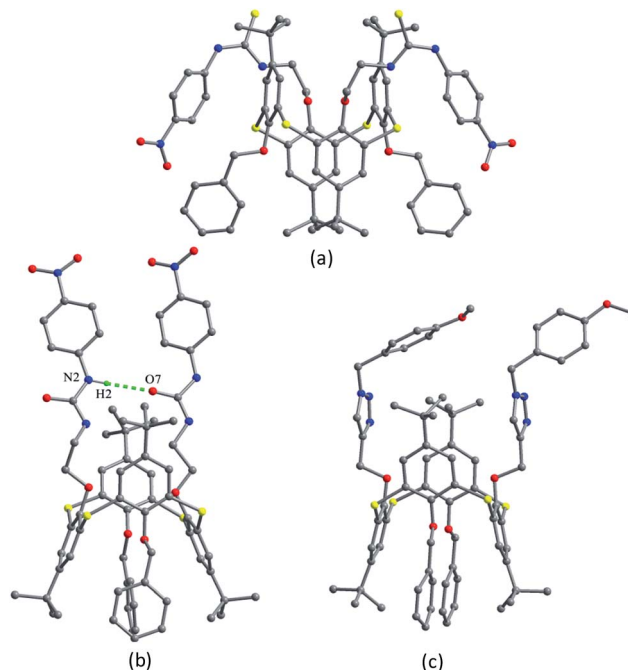


Fig. 67 Crystal structures of **71** (a), **72** (b) and **73** (c).

found that all three NH units of one chain act as a donor to form four intermolecular N–H...O H-bonds with one urea carbonyl O atom of the other chain and two ether O atoms, and thus the two urea units approach each other in a nearly parallel orientation. In solution, compound **74** can be employed as a ditopic receptor for molecular recognition based on the positive and negative allosteric effects.

In the structure of **75** (Fig. 70), two phenothiazine rings show a butterfly shape and produce a weak intramolecular C–H... $\pi$  contact. In the packing, a molecular dimer is formed by weak  $\pi$ – $\pi$  stacking contacts between two face-to-face paralleled phenothiazine rings of adjacent molecules (Fig. 71). Compound **75** exhibits a strong fluorescence emission with a large Stokes shift, which can be quenched selectively by Fe<sup>3+</sup> and Cr<sup>3+</sup> ions in solution.

Thiocalix[4]arene derivative **76** (Fig. 69),<sup>73</sup> functionalized with two nitrobenzofurazan (NBD) groups, crystallizes in a 1,3-alternate conformation with similar  $\theta$  values to **74** and **75**. Interestingly, the two NBD rings, one of which faces outward yielding an N–H...S H-bond, create a dihedral angle of 135.3°

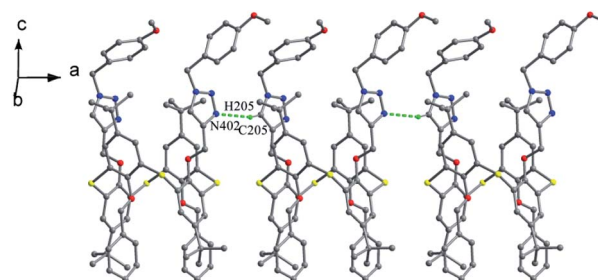


Fig. 68 Partial packing structure of **73**, showing a 1-D chain.



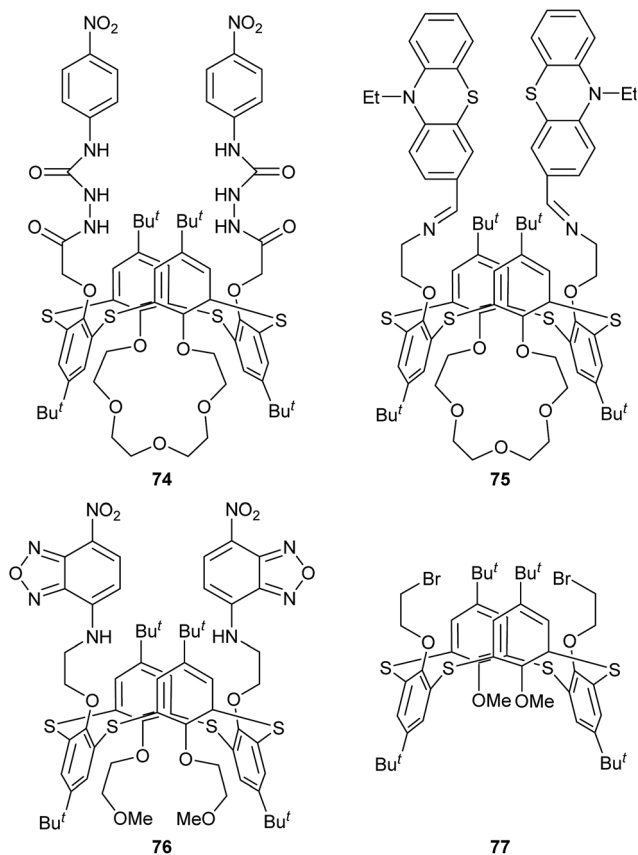
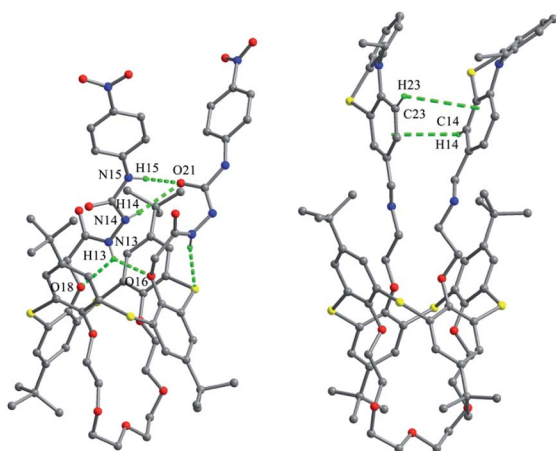


Fig. 69 Structures of compounds 74–77.

Fig. 70 Crystal structures of 74 (left) showing H-bonds, and 75 (right) showing C–H $\cdots$  $\pi$  contacts.

(Fig. 72). Due to the introduction of NBD groups, this compound can be applied as a colorimetric and fluorescence sensor for detection of  $\text{Ag}^+$  and  $\text{AcO}^-$  in solution.

Thiacalix[4]arene derivative 77 (Fig. 69),<sup>74</sup> with two OMe and two  $\text{OCH}_2\text{CH}_2\text{Br}$  arms, gives a 1,3-alternate conformation with two pairing  $\theta$  angles of 100.9 and 102.9° (Fig. 72). In the packing, a 1-D chain based on intermolecular  $\text{Br}\cdots\text{Br}$  contacts is

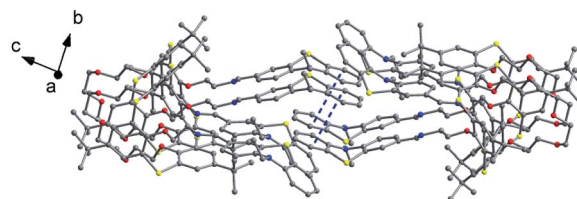
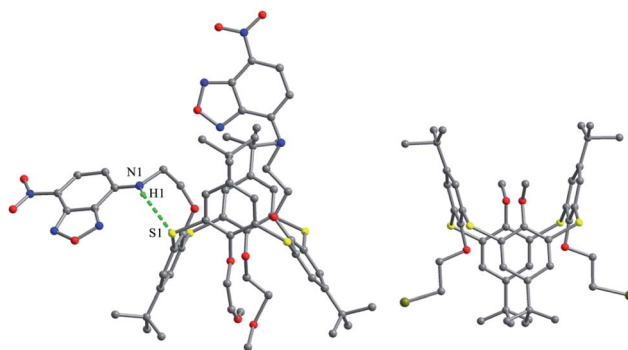
Fig. 71 Partial packing structure of 75, showing  $\pi$ – $\pi$  stackings.

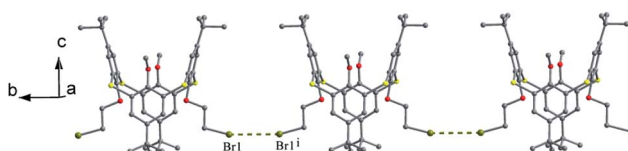
Fig. 72 Crystal structures of 76 (left) and 77 (right).

generated with an inter-halogen distance of 3.81 Å (Fig. 73), which is less than the sum of the van der Waals radii.

### 3.4 O/aryl mixed substituted thiacalix[4]arenes

In some cases, chemical modification of thiacalix[4]arenes can be performed at both the lower rim and the calix aryl rings to create new type of O/aryl substituted thiacalix[4]arenes. Hamada *et al.* have synthesized a series of such a type of thiacalix[4]arenes 78–89 (Fig. 74),<sup>75–78</sup> and studied extensively on their halogen interactions, revealing important insights into the formation of molecular assemblies in the solid state.<sup>10</sup> These compounds, except for 79 (see 112 in Section 5.2), all take a 1,3-alternate conformation with similar  $\theta$  values (Table 2), while they exhibit remarkably different assemblies due to the varied length of alkyl chain (methyl to decyl) at the lower rim.

Brominated thiacalix[4]arene 78 (Fig. 75a), with the smallest methyl groups, prefers to yield  $\text{Br}\cdots\pi$  contacts between distinct molecules. In its packing, symmetric expansion of molecules assembles into a layer-supramolecular structure with  $\text{Br}\cdots\pi$  and  $\text{C-H}\cdots\pi$  interactions (Fig. 76). In the case of molecule 80 (Fig. 75b), bearing *n*-propyl groups, a hexameric ring (Fig. 77), with a cyclohexane molecule enclosed, is formed by combining intermolecular  $\text{C-H}\cdots\text{S}$  H-bonds,  $\pi$ – $\pi$  and  $\text{S}\cdots\pi$  interactions

Fig. 73 Partial packing structure of 77, showing a 1-D chain based on  $\text{Br}\cdots\text{Br}$  contacts.

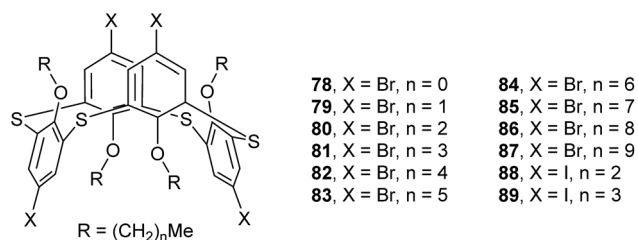


Fig. 74 Structures of compounds 78–89.

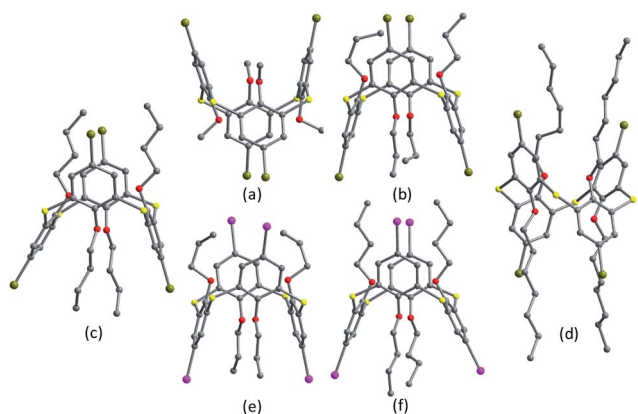
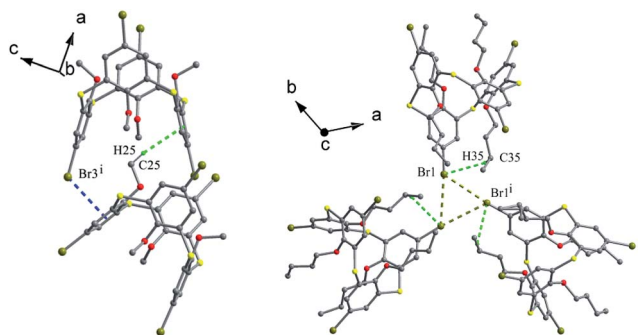
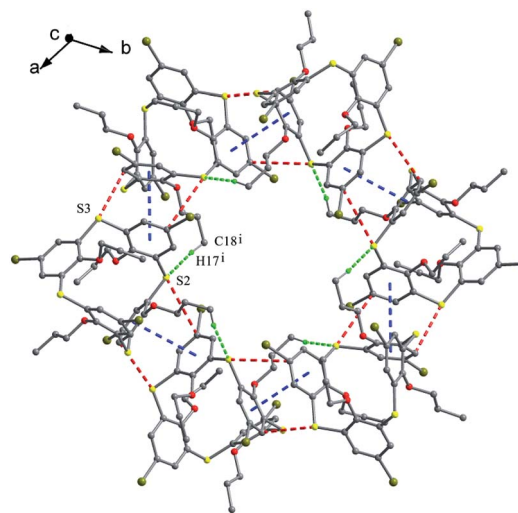


Fig. 75 Crystal structures of 78 (a), 80 (b), 81 (c), 84 (d), 88 (e) and 89 (f).

between vicinal molecules. Molecule **81** (Fig. 75c) possesses moderate *n*-butyl chains and offers a skewed 1,3-alternate conformation with a  $\theta$  range of 103.1–123.0°, which is favored to create intermolecular Br $\cdots$ Br interactions in the crystalline state. Thus an infinite open-network is generated with six trimeric units through triangular Br<sub>3</sub> motif halogen–halogen contacts and C35–H35 $\cdots$ Br<sub>4</sub> interactions (Fig. 76). However, such halogen interactions were not observed in the crystal structures of brominated thiacalix[4]arenes **80**, **82** and **83**.

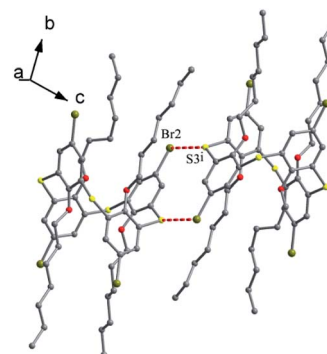
In comparison, brominated thiacalix[4]arene derivatives **84**–**87**, bearing longer chains, are favored to assemble *via* Br $\cdots$ S halogen bonding. Molecule **84** with larger *n*-heptyl groups (Fig. 75d), for instance, demonstrates Br $\cdots$ S contacts as the *n*-

Fig. 76 A dimer of **78** (left) built by Br $\cdots$  $\pi$  and C–H $\cdots$  $\pi$  contacts, and a triangular Br<sub>3</sub> motif of **81** (right) formed by Br $\cdots$ Br and C–H $\cdots$ Br interactions.Fig. 77 A hexameric assembly of **80**, showing intermolecular  $\pi$ – $\pi$  (blue), S $\cdots$  $\pi$  (red) and C–H $\cdots$ S (green) interactions.

heptyl chain blocks Br atom from interacting with other halogens or aromatic rings (Fig. 78).

Thiacalix[4]arenes **88** (Fig. 75e) and **89** (Fig. 75f) have four I atoms at the upper rim. In the packing of **88**, intermolecular I $\cdots$ I, S $\cdots$  $\pi$  and C–H $\cdots$ I interactions were demonstrated in the supramolecular assembly (Fig. 79), which is produced *via* preferential I $\cdots$ I interactions. However, in the case of **89**, a supramolecular assembly is yielded by S $\cdots$ I and C–H $\cdots$ S bonding, together with weak S $\cdots$  $\pi$  and C–H $\cdots$ I interactions (Fig. 79). It should be noted that iodine-containing thiacalix[4]arenes have stronger interactions involving iodine than bromine as the former possesses a stronger polarizing power than the latter.

Tetrapropoxythiacalix[4]arene derivatives **90** (ref. 79) and **91** (ref. 80) (Fig. 80), mono-functionalized at the *m*-position, both exhibit a 1,3-alternate conformation with four similar  $\theta$  angles (Table 2). In the packing of **90**, a unique dimer is yielded through Br $\cdots$  $\pi$  interactions between bromine atoms and phenolic rings of the neighboring molecules (Fig. 81). In the case of **91**, two NH units of the ureido group at the *m*-position create two asymmetric H-bonds with the O atom of THF (Fig. 82). In addition, two *p*-nitrophenylureido moieties are

Fig. 78 A dimer of **84**, showing Br $\cdots$ S interactions.

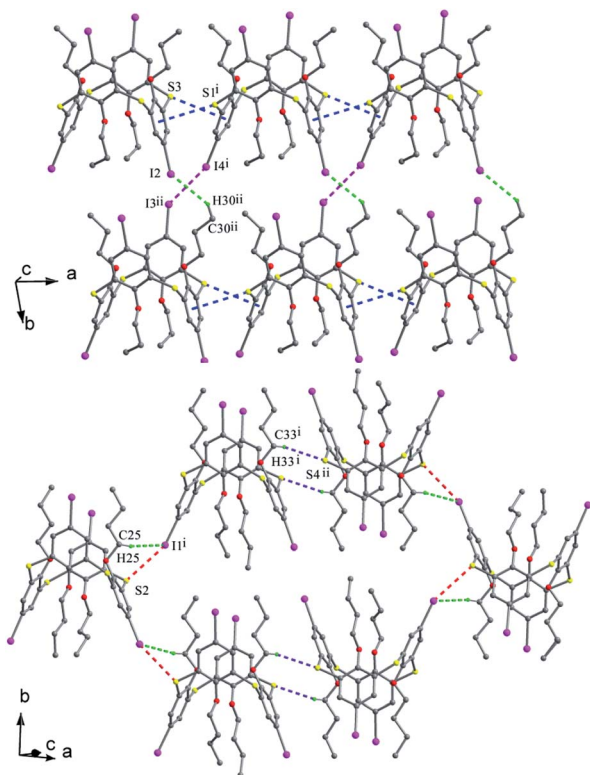


Fig. 79 Supramolecular assemblies of **88** (top) built by I...I (pink), C-H...I (green) and S... $\pi$  (blue) interactions, and **89** (bottom) built by I...S (red), C-H...I (green) and C-H...S (purple) interactions.

strictly coplanar to each other, producing a dimer by intermolecular  $\pi$ - $\pi$  interactions.

Tetrapropoxythiacalix[4]arenes **92** and **93** (Fig. 80),<sup>81</sup> *m*- and *p*-monomercurated regioisomers, are in a 1,3-alternate or cone conformer. In the asymmetric unit of **92**, there are two pinched cone conformers with  $\theta$  ranges of 66.1–154.6° in A (HgCl unit orienting outside the cavity) and 72.8–155.9° in B (HgCl unit orienting inside the cavity) (Fig. 83a). In addition, it also gives a 1,3-alternate conformer with a  $\theta$  range of 111.0–114.6° (Fig. 83b). The aromatic rings bearing the HgCl group at the *m*-position are parallel to each other and yield a dimer by cation- $\pi$  interactions (Fig. 84). And the Hg atoms locate exactly above the centroid of the parallel aromatic ring from the vicinal molecules. But for **93**, it is only in a 1,3-alternate conformation with a  $\theta$  range from 111.4 to 115.9° (Fig. 83c). An interesting motif can be found in the crystal packing of **93**, where the intermolecular Hg...Cl interactions lead to the formation of a dimer

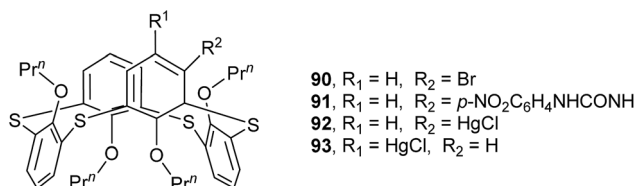


Fig. 80 Structures of compounds **90**–**93**.

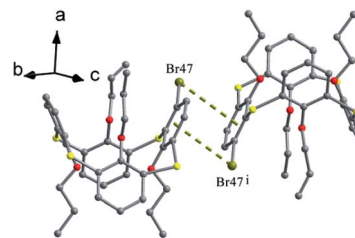


Fig. 81 A dimer of **90** formed with Br... $\pi$  interactions.

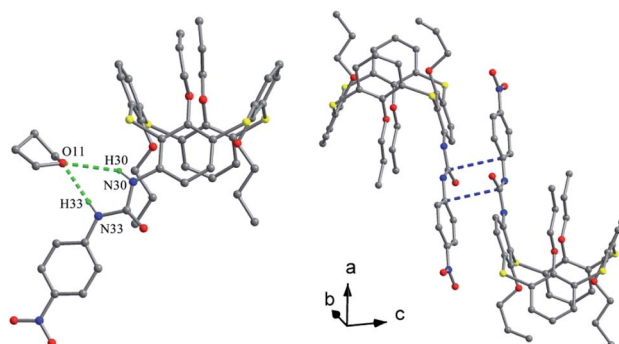


Fig. 82 Crystal structure of **91** (left) showing H-bonds with THF molecule, and a dimer of **91** (right) showing  $\pi$ - $\pi$  interactions.

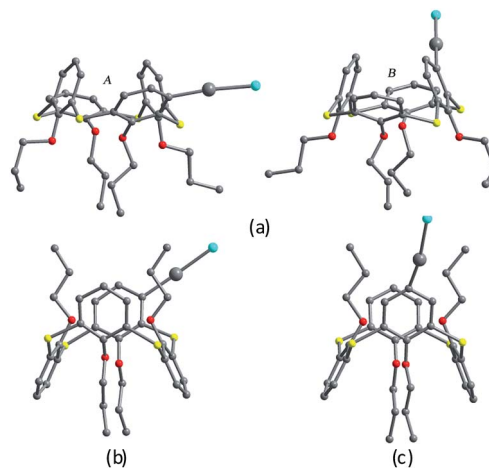


Fig. 83 Crystal structures of **92** in cone (A and B) (a), in 1,3-alternate (b), and **93** (c).

(Fig. 84), which is further strengthened by additional C-H...Cl H-bonds between the HgCl unit and the aromatic ring.

In summary, the geometry of thiacalix[4]arenes in a 1,3-alternate conformation differs essentially from those in a cone conformer. Most 1,3-alternate thiacalix[4]arenes may be divided into three types based on the  $\theta$  variants: (1) with the same four  $\theta$  angles, (2) with two pairs of  $\theta$  angles, and (3) with four similar  $\theta$  angles. The 1,3-alternate conformation is also stabilized by the intramolecular H-bonds and weak contacts similar to the cone conformer. In the packing, the most important feature is that the thiacalix[4]arene core and its pendant groups facilitate the



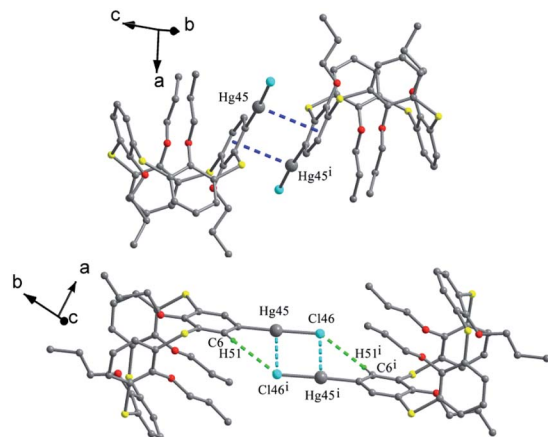


Fig. 84 Dimers of **92** (top) and **93** (bottom).

formation of more complex supramolecular assemblies with branched intermolecular interactions. Especially, various hetero atoms in these compounds can offer more chances in creating diverse kinds of interactions. Therefore various motifs and beautiful channels are constructed by aggregation of the host molecules.

## 4. 1,2-Alternate structures of thiacalix[4]arenes

As of now, only few of thiacalix[4]arene derivatives shows a 1,2-alternate conformation, usually with a centrosymmetry as their four phenolic rings locate in two opposite sides.

### 4.1 O-Substituted thiacalix[4]arenes

In general, the distally substituted calix[4]arene derivatives prefer a cone conformation in the solid state, while the corresponding thiacalix[4]arene derivatives may adopt either a cone or a 1,2-alternate conformer.

Lhoták *et al.* have studied the conformational behavior of a series of such thiacalix[4]arenes **94–99** (Fig. 85).<sup>44,82</sup> In the solid state, **94–96** and **98** take a 1,2-alternate conformation with approximate (**94**) or complete centrosymmetry (**95**, **96**, and **98**) with similar  $\theta$  ranges (Table 3). This kind of conformers is governed by two H-bonds between OH and alkoxy groups of the adjacent aromatic rings. They create a novel type of molecular channels held together by  $\pi$ - $\pi$  interactions. For instance, molecule **94** (Fig. 86a),<sup>82</sup> a dimethoxy derivative of thiacalix[4]arene, shows a 1,2-alternate conformation fixed mainly by two intramolecular O-H $\cdots$ O H-bonds between the OH and OMe groups. Moreover, two intramolecular O-H $\cdots$ S H-bonds are yielded between the OH and S moieties. In the packing, a dimer is built by intermolecular  $\pi$ - $\pi$  interactions between the aromatic rings (Fig. 86b). Further expansion of these dimers generates an infinite molecular channel (Fig. 86c). In addition, the 1,2-alternate conformers of **95** (with ethoxy groups) and **96** (with *n*-propoxy groups) are further stabilized by intramolecular C-H $\cdots$  $\pi$  interactions between the alkoxy and the neighboring inverted aromatic ring. However, different conformational properties of

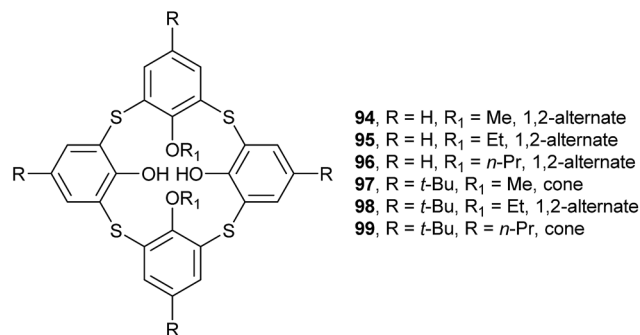


Fig. 85 Structures of compounds **94–99**.

Table 3 The  $\theta$  angles of compounds **94–105**<sup>a</sup>

Compd.	$\theta$ ( $^\circ$ )			
<b>94</b>	113.8	129.9	114.3	131.9
<b>95</b>	121.4	123.8	121.4	123.8
<b>96</b>	115.8	126.5	115.8	126.5
<b>97</b>	73.2	134.9	110.8	135.8
<b>98</b>	116.6	121.2	116.6	121.2
<b>99</b>	72.0	155.6	107.1	141.6
<b>100</b>	105.3	114.5	105.3	114.5
<b>101</b>	118.8	130.9	118.8	130.9
<b>102</b>	102.9	167.0	102.9	167.0
<b>103</b>	106.8	123.6	106.8	123.6
<b>104</b>	111.7	114.7	111.7	114.7
<b>105</b>	116.1	132.4	116.1	132.4

<sup>a</sup> Data obtained by calculation with Diamond Version 3.0.

**97** and **99**, with *t*-butyl at the upper rim, were found in a pinched cone conformation, in which both free OH groups interact with the same ether O atom. Interestingly, molecule **96** also exists in a cone conformer described above (see **29** in Section 2.3), due to the introduction of bulkier *n*-propyl groups than methyl and ethyl groups in **94** and **95**, respectively.

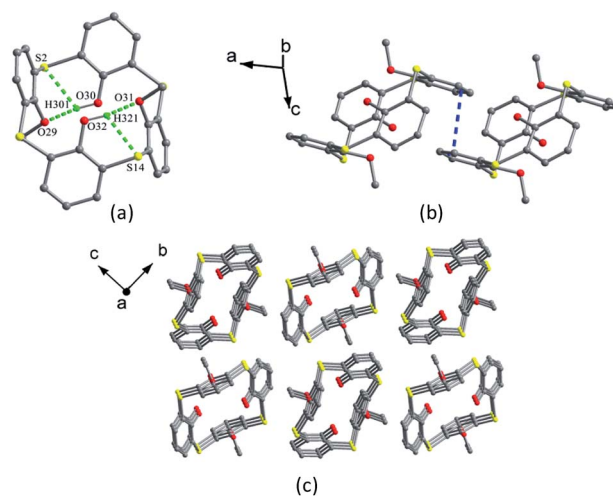


Fig. 86 Crystal structure of **94** (a) showing O-H $\cdots$ O and O-H $\cdots$ S H-bonds, a dimer of **94** (b) built *via*  $\pi$ - $\pi$  interactions, and partial packing structure of **94** (c) showing the molecular channels.



Thiacalix[4]arene derivatives **100**–**103** (Fig. 87), all adopt a centrosymmetric 1,2-alternate conformation with two pairs of  $\theta$  angles (Table 3), and their opposite inverted aromatic rings are nearly parallel. In the crystal structure of **100** (Fig. 88a),<sup>83</sup> bearing four *n*-propoxy groups at the lower rim, no intramolecular H-bond was observed as in **96** (with two *n*-propoxy groups), due to the absence of OH groups. However, an infinite channel is still yielded with molecules being packed parallel to each other (Fig. 89).

Thiacalix[4]arene derivative **101** (Fig. 88b),<sup>84</sup> with two nitro and two *n*-propoxy groups at the upper and lower rims, respectively, is also stabilized by two intramolecular H-bonds between the OH and the ether O atoms, which is similar to **96**. Differently, in the packing, a centrosymmetric dimer is formed by two C–H...O H-bonds between the nitro O atom and the phenolic *meta*-H atom of the vicinal molecules (Fig. 90).

In addition, some other ancillary forces can also stabilize the 1,2-alternate conformer of thiacalix[4]arenes. Molecule **102** (Fig. 88c),<sup>85</sup> a phosphorylation derivative of **1**, is in a flattened 1,2-alternate conformation. Such a flattened structure is fixed by intramolecular weak P...S and P–Cl... $\pi$  interactions, leading one couple of opposite aromatic rings being nearly parallel to the *R* plane.

In the crystal structure of **103** (Fig. 88d),<sup>86</sup> bearing four 2-cyanobenzoyloxy units at the lower rim, the two pairs of distal cyanophenyl rings are nearly parallel with the same dihedral angle of 7.3°, owing to the formation of intramolecular  $\pi$ – $\pi$  interactions between them.

## 4.2 Aryl-functionalized thiacalix[4]arenes

Thiacalix[4]arene derivatives **104** (ref. 87) and **105** (ref. 88) (Fig. 91), modified with four functions at the upper rim, both show a 1,2-alternate conformation with centrosymmetry, indicating that facing inverted phenolic rings are parallel to each other with two pairs of  $\theta$  values (Table 3). In the solid state, the typical cyclic intramolecular H-bonds disappear, but other H-bonds were observed in the 1,2-alternate conformer. In

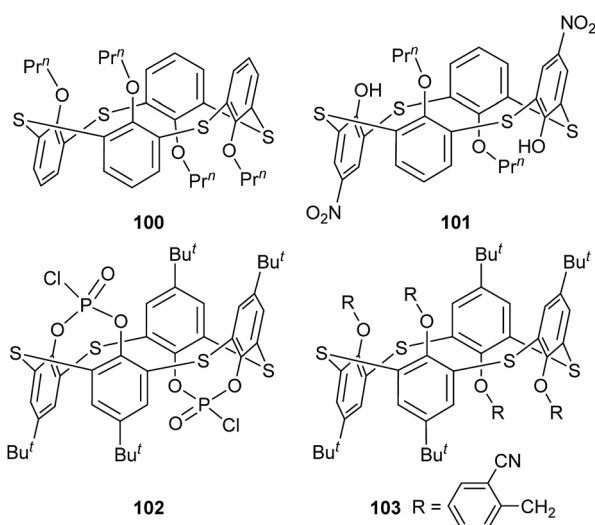


Fig. 87 Structures of compounds **100**–**103**.

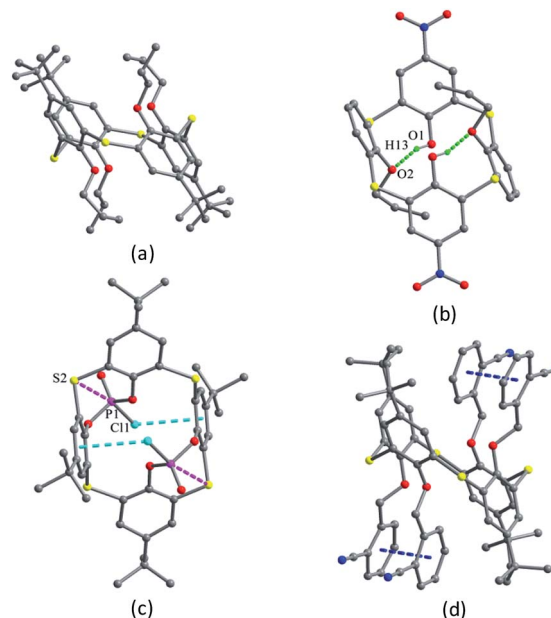


Fig. 88 Crystal structures of **100** (a), **101** (b), **102** (c) and **103** (d), showing P...S (pink), P–Cl... $\pi$  (cyan), and  $\pi$ ... $\pi$  (blue) interactions.

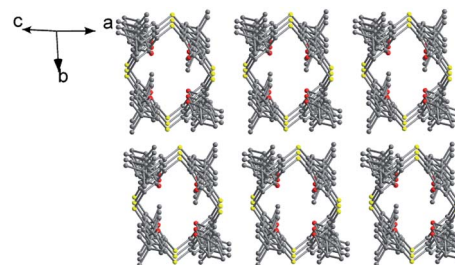


Fig. 89 Partial packing structure of **100**, showing the molecular channels.

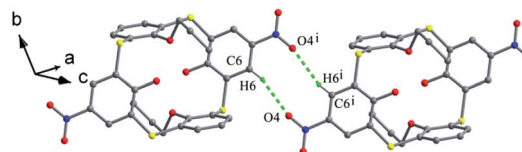


Fig. 90 A dimer of **101**, showing C–H...O H-bonds.

molecule **104** (Fig. 92), four intramolecular O–H...S H-bonds are yielded between the S bridge and its two vicinal OH groups at the same side. Moreover, there are strong intermolecular O14–H14...O50 and O13–H13...O50 H-bonds with two DMSO guest molecules.

In the case of **105** (Fig. 92), with four *p*-nitrophenylazo functions at the upper rim, only two intramolecular O–H...O H-bonds govern such a conformation rather than the annular H-bond array, while the other two OH groups create two O–H...N H-bonds with the solvent pyridine molecules crystallized in the crystal structure. Moreover, intramolecular O–H...S H-bonds and O...S contacts were also found.





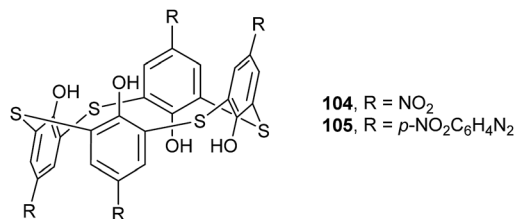
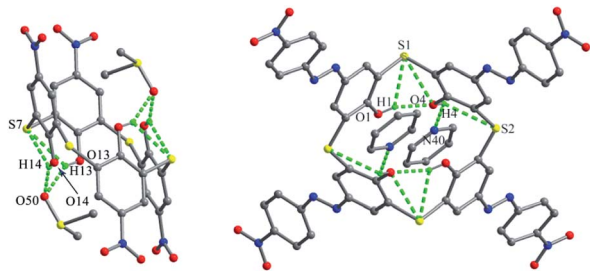


Fig. 91 Structures of compounds 104–105.

Fig. 92 Crystal structures of **104** (left) and **105** (right), showing intra- and intermolecular H-bonds with the solvent molecules.

In brief, identically substituted thiacalix[4]arenes in a 1,2-alternate conformer usually show centrosymmetry with two pairs of  $\theta$  values. In such an unusual 1,2-alternate conformer, it is hard to create a cycle of intramolecular O–H $\cdots$ O H-bonds with four free OH groups, which always exist in the cone conformer. However, the intramolecular O–H $\cdots$ O H-bonds are still a key interaction to control the 1,2-alternate conformation. In the packing, the orientations of four phenolic rings at two opposite sides are usually favored to stack parallel to each other and yield the infinite channels.

## 5. Partial cone structures of thiacalix[4]arenes

In partial cone thiacalix[4]arene derivatives, one of the four phenolic rings is rotated away from the cavity formed by the other three phenolic rings, thus they are all unsymmetrical molecules.

### 5.1 O-Substituted thiacalix[4]arenes

Thiacalix[4]arene derivatives **106–108** possess four ether arms terminated with amide or ester groups at the lower rim (Fig. 93).<sup>89</sup> In the solid state, they all take a partial cone conformer, in which the inverted aromatic ring is nearly perpendicular to the *R* plane with  $\theta$  angles of 86.6–90.4° (Table 4). In molecule **106** (Fig. 94a), containing two amide and two ester termini, the ester carbonyl group on the inverted aromatic ring is orientated inwards the cavity, while the other one is directed outwards. This conformer is favorable to give an intramolecular N–H $\cdots$ O H-bond between the ester carbonyl group and the vicinal amide unit. In the case of **107** (Fig. 94b), although the ester group on the inverted phenolic ring is replaced by an amide group, it adopts a similar conformation and gives the same intramolecular N–H $\cdots$ O H-bond as in **106**. In the packing, similar infinite chains are produced in **106**

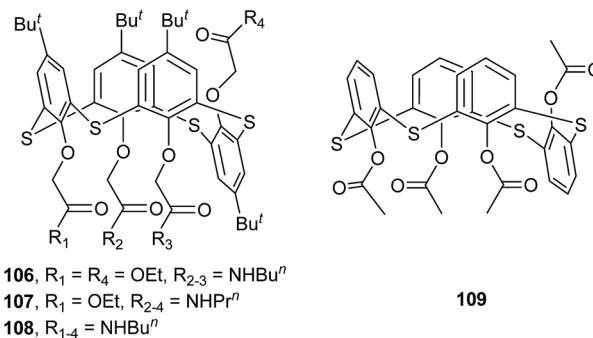


Fig. 93 Structures of compounds 106–109.

(Fig. 95a) and **107** (Fig. 95b) by intermolecular N–H $\cdots$ O H-bonds between the amide groups of two vicinal molecules. In addition, such chains in **107** are further linked into supramolecular arrays by inter-chain N–H $\cdots$ O H-bonds with the NH groups on the inverted phenolic rings as H-bond donors. However, molecule **108**, bearing four amide groups (Fig. 94c), displays a partial cone conformation with the  $\theta$  range of 80.3–155.0° larger than those in **106** and **107**. In such a conformer, all carbonyls of the amide groups are directed away from the cavity, with two intramolecular N–H $\cdots$ O H-bonds between the three amide groups at the same side. This H-bonding nature is different from that observed in **106** and **107**. In the packing, a zigzag 1-D infinite chain is created by intermolecular N–H $\cdots$ O H-bonds (Fig. 95c). In solution, it was observed that only **108** exhibited some affinity towards Na<sup>+</sup> and K<sup>+</sup> ions.

In the asymmetric unit of tetraacetylated thiacalix[4]arene **109** (Fig. 93),<sup>90</sup> there are one thiacalix[4]arene molecule and one CHCl<sub>3</sub> solvent molecule. In the packing, a structural motif is formed, in which one thiacalix[4]arene is surrounded by four CHCl<sub>3</sub> molecules and *vice versa*. The CHCl<sub>3</sub> molecule is bound by intermolecular C–H $\cdots$ O, C–H $\cdots$ Cl and Cl $\cdots$ O interactions with its adjacent thiacalix[4]arene molecules. In addition, strong intermolecular  $\pi$ – $\pi$  contacts were found between two parallel phenyl rings, giving rise to a dimer (Fig. 96), which was further fixed by C–H $\cdots$ O H-bonds between the carbonyl group and the H atom at the *m*-position of the opposite phenyl ring.

### 5.2 O/aryl mixed substituted thiacalix[4]arenes

Thiacalix[4]arene derivative **110** (Fig. 97),<sup>45</sup> with one *n*-propoxy at the lower rim and three CHO functions at the upper rim,

Table 4 The  $\theta$  angles of compounds 106–113<sup>a</sup>

Compd.	$\theta$ (°)			
<b>106</b>	90.4	88.0	138.9	94.5
<b>107</b>	88.4	95.0	142.1	84.5
<b>108</b>	88.4	80.3	155.0	123.2
<b>109</b>	86.6	82.0	145.8	79.5
<b>110</b>	90.1	101.4	136.8	106.5
<b>111</b>	103.6	99.3	153.9	106.6
<b>112</b>	93.0	85.5	152.0	81.1
<b>113</b>	82.4	86.0	162.5	75.7

<sup>a</sup> Data obtained by calculation with Diamond Version 3.0.



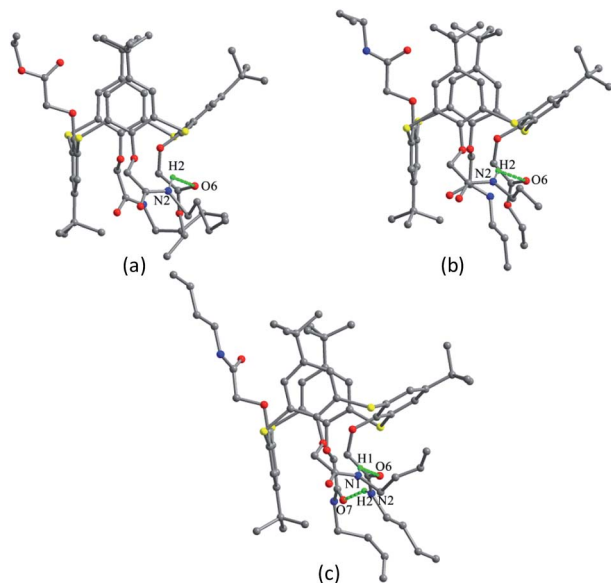


Fig. 94 Crystal structures of 106 (a), 107 (b) and 108 (c), showing H-bonds.

takes a partial cone conformer, in which the inverted aromatic ring is perpendicular to the *R* plane with  $\theta$  value of  $90.1^\circ$  (Table 4). Such a conformer is fixed by intramolecular O-H $\cdots$ O and O-H $\cdots$ S H-bonds (Fig. 98). In the packing, two molecules of **110**

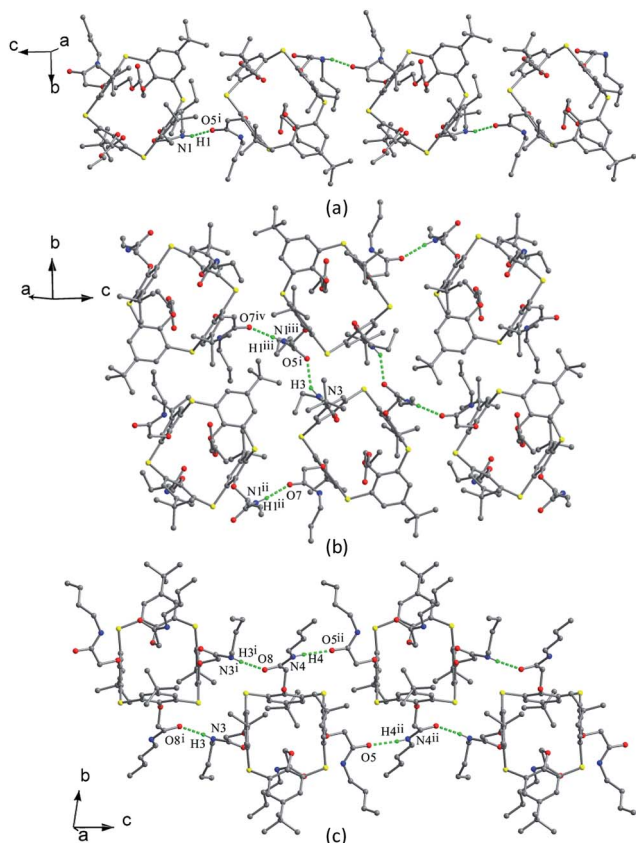


Fig. 95 Partial stacking structures of 106 (a), 107 (b) and 108 (c) built by H-bonds.

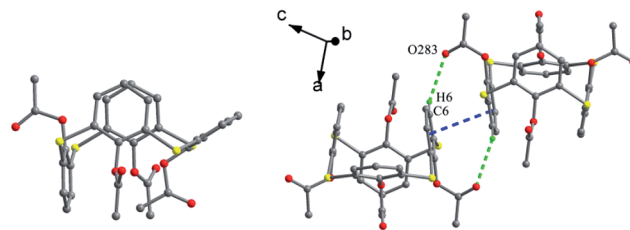


Fig. 96 Crystal structure of 109 (left), and a dimer of 109 (right) built by C-H $\cdots$ O and  $\pi$ - $\pi$  interactions.

form a head-to-head dimer by  $\pi$ - $\pi$  stacking between the parallel aromatic rings, two weak C-H $\cdots$ O H-bonds and four C-H $\cdots$  $\pi$  interactions (Fig. 99). In addition, six molecules of **110** create a hexameric disc in a back-to-back fashion by S3 $\cdots$  $\pi$  and C29-H29 $\cdots$ O6 interactions (Fig. 100). These discs are further accumulated into a triply helical tube, which is stabilized by C-O $\cdots$  $\pi$  and C-H $\cdots$ O interactions.

Tripropoxythiacalix[4]arene derivative **111** (Fig. 97),<sup>91</sup> with a ClCH<sub>2</sub> group at the *m*-position, shows a partial cone conformer with four different  $\theta$  values (Table 4). Two intramolecular O-H $\cdots$ O H-bonds between the OH and two *n*-propoxy groups at the same side control the strong distortion of the conformer (Fig. 98).

Thiacalix[4]arene derivatives **112** (ref. 78) and **113** (ref. 92) (Fig. 97), functionalized with four Br atoms at the upper rim, both take a partial cone conformation with inverted aromatic ring nearly perpendicular to the plane *R* in the solid state (Table 4). For compound **112** (Fig. 101), appending four ethyl groups at the lower rim, two facing rings of the three aromatic rings on the same side are flipped slightly inwards, whereas the middle one is flipped considerably outwards. Such a conformer lets a short Br $\cdots$  $\pi$  and two C-H $\cdots$ Br interactions contribute to the formation of the self-assembled dimer (Fig. 99). In addition, symmetric expansion of the crystal structure shows S $\cdots$  $\pi$  and C-H $\cdots$ S contacts between the dimers.

In the case of **113** (Fig. 101), bearing four ether chains terminated with ester groups, the ring on the opposite of the

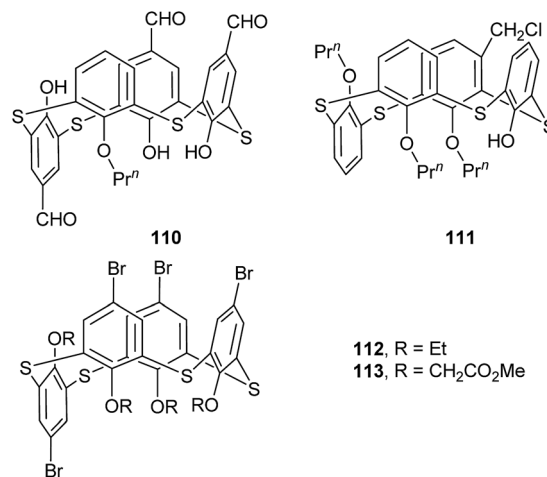


Fig. 97 Structures of compounds 110–113.



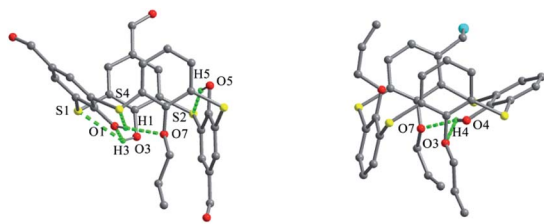


Fig. 98 Crystal structures of **110** (left) and **111** (right), showing H-bonds.

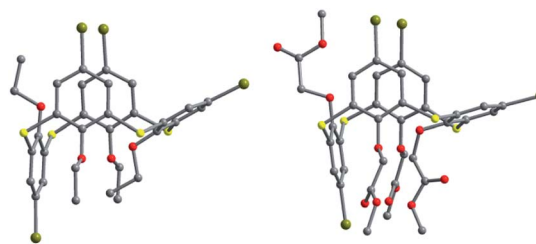


Fig. 101 Crystal structures of **112** (left) and **113** (right).

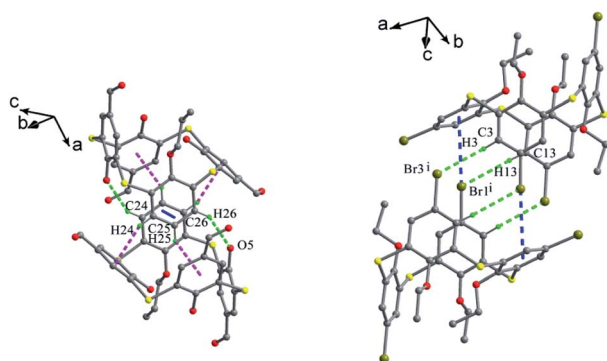


Fig. 99 A dimer of **110** (left) built by  $\pi$ - $\pi$  (blue), C-H $\cdots$ O (green) and C-H $\cdots$  $\pi$  (pink) interactions; a dimer of **112** (right) built by Br $\cdots$  $\pi$  (blue) and C-H $\cdots$ Br (green) interactions.

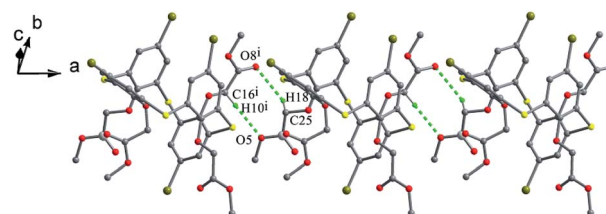


Fig. 102 A 1-D chain of **113** built by C-H $\cdots$ O H-bonds.

available for the formation of intra- and intermolecular interactions, which are able to stabilize both the partial cone conformers and their supramolecular arrays.

## 6. Conclusions

In conclusion, we have briefly summarized the development of thiacalix[4]arene derivatives in crystal structures, including the exact description of various conformers, binding patterns and some supramolecular assemblies.

In the solid state, thiacalix[4]arenes, in cone, 1,3-alternate, 1,2-alternate and partial cone conformations, show diverse conformational preferences with varied substituents at the lower and/or upper rims, as well as the oxidation of the S bridges. The precise conformations of thiacalix[4]arene cores can be identified with the typical  $\theta$  angles. In each type of conformers, the  $\theta$  ranges are very different owing to the features of the substituents. The whole molecular structures are mainly governed by the steric and electronic effects of the substituents belonging to the thiacalix[4]arene molecules and the crystallization conditions.

In the crystal structures of thiacalix[4]arenes, various X-H $\cdots$ Y (X = O, N, C; Y = O, N, S, Cl, Br, I) H-bonds, C-H $\cdots$  $\pi$ ,  $\pi$ - $\pi$ , X $\cdots$  $\pi$  (X = S, Cl, Br) and X $\cdots$ X (X = S, Cl, Br, I) interactions as well as other contacts between different heteroatoms are found to control the whole molecular conformations and stabilize the supramolecular assemblies. In particular, the introduction of S bridges offers additional binding centres for H-bonds and other non-covalent contacts. Moreover, the solvent molecules play an ancillary role in regulating the conformation and the packing of thiacalix[4]arenes in some cases by two ways: one is guest inclusion occurring in the calix cavity; the other occurs in the holes or channels built by aggregation of the host molecules.

In the supramolecular assemblies, versatile multimeric motifs, chain and channel arrays of thiacalix[4]arenes are

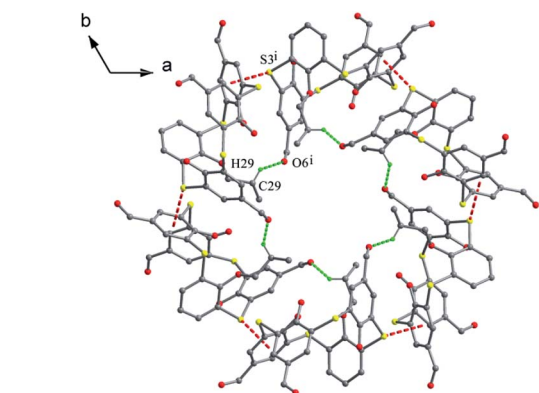


Fig. 100 A disc-like hexamer of **110** built by C-H $\cdots$ O and S $\cdots$  $\pi$  interactions.

inverted one is tilted away from the cavity and almost coplanar with the *R* plane. In the crystal structure, C-H $\cdots$ O, C-H $\cdots$ S and C-H $\cdots$  $\pi$  interactions fix both the partial cone conformer and the packing. A 1-D chain is created by intermolecular C-H $\cdots$ O H-bonds (Fig. 102). These chains further augmented into a 2-D network *via* ancillary C-Br $\cdots$ C interactions.

As shown above, for most of thiacalix[4]arenes in a partial cone conformation, the inverted phenolic ring is almost perpendicular to the *R* plane with the  $\theta$  range from 80.3 to 103.6°, while its opposing ring is markedly tilted away from the cavity with the  $\theta$  range from 136.8 to 162.5° (Table 4). These partial cone conformers tailored with different binding sites are



created *via* the interactions described above. In particular, those in cone and 1,3-alternate conformers always display square box-shaped cavities and yield very nice infinite channels, which are extensively influenced with the features of substituents at the lower and/or upper rims. These supramolecular arrays are widely favored to allow inclusion or storage of small molecules with complementary size.

In this review, we have highlighted some of the promising advances of thiacalix[4]arenes in crystallographic researches, but it is clear that there is a long path ahead of to develop the perfect thiacalix[4]arene-based supramolecular assemblies. In the future, more attention should be paid to expand the areas involving design of novel molecules, discovery of new interactions and establishment of the rule in molecular recognition and organic supramolecular assemblies based on the thiacalix [4]arene scaffolds. Understanding well the crystal structures of these scaffolds will provide wide applications in biological molecular recognition, functional organic materials and supramolecular chemistry.

## Acknowledgements

We are grateful for the financial support from the National Natural Science Foundation of China (No. 21372147).

## References

- 1 S. Shinkai, *Tetrahedron*, 1993, **49**, 8933–8968.
- 2 C. D. Gutsche, in *Calixarenes Revisited, Monographs in Supramolecular Chemistry*, ed. J. F. Stoddart, The Royal Society of Chemistry, Cam Cambridge, 1989.
- 3 H. Kumagai, M. Hasegawa, S. Miyanari, Y. Sugawa, Y. Sato, T. Hori, S. Ueda, H. Kamiyama and S. Miyano, *Tetrahedron Lett.*, 1997, **38**, 3971–3972.
- 4 T. Sone, Y. Ohba, K. Moriya, H. Kumada and K. Ito, *Tetrahedron*, 1997, **53**, 10689–10698.
- 5 E. A. Shokova and V. V. Kovalev, *Russ. J. Org. Chem.*, 2003, **39**, 1–28.
- 6 N. Iki and S. Miyano, *J. Inclusion Phenom. Macrocyclic Chem.*, 2001, **41**, 99–105.
- 7 P. Lhoták, *Eur. J. Org. Chem.*, 2004, 1675–1692.
- 8 N. Morohashi, F. Narumi, N. Iki, T. Hattori and S. Miyano, *Chem. Rev.*, 2006, **106**, 5291–5316.
- 9 R. Kumar, Y. O. Lee, V. Bhalla, M. Kumar and J. S. Kim, *Chem. Soc. Rev.*, 2014, **43**, 4824–4870.
- 10 M. Yamada, M. R. Gandhi, U. M. R. Kunda and F. Hamada, *J. Inclusion Phenom. Macrocyclic Chem.*, 2016, **85**, 1–18.
- 11 T. Kajiwara, N. Iki and M. Yamashita, *Coord. Chem. Rev.*, 2007, **251**, 1734–1746.
- 12 Y. Bi, S. Du and W. Liao, *Coord. Chem. Rev.*, 2014, **276**, 61–72.
- 13 A. Bilyk, A. K. Hall, J. M. Harrowfield, M. W. Hosseini, B. W. Skelton and A. H. White, *Inorg. Chem.*, 2001, **40**, 672–686.
- 14 A. Bilyk, J. W. Dunlop, A. K. Hall, J. M. Harrowfield, M. W. Hosseini, G. A. Koutsantonis, B. W. Skelton and A. H. White, *Eur. J. Inorg. Chem.*, 2010, **14**, 2089–2105.
- 15 Y. Li, W. Yang, Y. Chen and S. Gong, *CrystEngComm*, 2011, **13**, 259–268.
- 16 H. Akdas, L. Bringel, E. Graf, M. W. Hosseini, G. Mislin, J. Pansanel, A. D. Cian and J. Fischer, *Tetrahedron Lett.*, 1998, **39**, 2311–2314.
- 17 J. Lang, K. Vágnerová, J. Czernek and P. Lhoták, *Supramol. Chem.*, 2006, **18**, 371–381.
- 18 N. Iki, C. Kabuto, T. Fukushima, H. Kumagai, H. Takeya, S. Miyanari, T. Miyashi and S. Miyano, *Tetrahedron*, 2000, **56**, 1437–1443.
- 19 N. Morohashi, S. Noji, H. Nakayama, Y. Kudo, S. Tanaka, C. Kabuto and T. Hattori, *Org. Lett.*, 2011, **13**, 3292–3295.
- 20 A. Arduini, F. F. Nachtigall, A. Pochini, A. Secchi and F. Ugozzoli, *Supramol. Chem.*, 2000, **12**, 273–291.
- 21 J. Hong, C. Yang, Y. Li, G. Yang, C. Jin, Z. Guo and L. Zhu, *J. Mol. Struct.*, 2003, **655**, 435–441.
- 22 C. Kabuto, Y. Higuchi, T. Niimi, F. Hamada, N. Iki, N. Morohashi and S. Miyano, *J. Inclusion Phenom. Macrocyclic Chem.*, 2002, **42**, 89–98.
- 23 P. Lhoták, T. Šmejkal, I. Stibor, J. Havlíček, M. Tkadlecová and H. Petříčková, *Tetrahedron Lett.*, 2003, **44**, 8093–8097.
- 24 O. Kasyan, V. Kalchenko, M. Bolte and V. Böhmer, *Chem. Commun.*, 2006, **18**, 1932–1934.
- 25 N. Morohashi, M. Kojima, A. Suzuki and Y. Ohba, *Heterocycl. Commun.*, 2005, **11**, 249–254.
- 26 H. Katagiri, S. Tanaka, K. Ohkubo, Y. Akahira, N. Morohashi, N. Iki, T. Hattori and S. Miyano, *RSC Adv.*, 2014, **4**, 9608–9616.
- 27 H. Katagiri, N. Iki, T. Hattori, C. Kabuto and S. Miyano, *J. Am. Chem. Soc.*, 2001, **123**, 779–780.
- 28 N. Morohashi, H. Katagiri, T. Shimazaki, Y. Kitamoto, S. Tanaka, C. Kabuto, N. Iki, T. Hattori and S. Miyano, *Supramol. Chem.*, 2013, **25**, 812–818.
- 29 S. Kharchenko, A. Drapailo, S. Shishkina, O. Shishkin, M. Karavan, I. Smirnov, A. Ryabitskii and V. I. Kalchenko, *Supramol. Chem.*, 2014, **26**, 864–872.
- 30 M. Lamouchi, E. Jeanneau, R. Chiriach, D. Ceroni, F. Meganem, A. Brioude, A. W. Coleman and C. Desroches, *Tetrahedron Lett.*, 2012, **53**, 2088–2090.
- 31 M. Akkurt, J. P. Jasinski, S. K. Mohamed, O. A. Omran and M. R. Albayati, *Acta Crystallogr., Sect. E: Crystallogr. Commun.*, 2015, **71**, o830–o831.
- 32 I. I. Stoikov, D. S. Ibragimova, N. V. Shestakova, D. B. Krivolapov, I. A. Litvinov, I. S. Antipin, A. I. Konovalov and I. Zharov, *Supramol. Chem.*, 2009, **21**, 564–571.
- 33 J.-L. Zhao, H. Tomiyasu, X.-L. Ni, X. Zeng, M. R. J. Elsegood, C. Redshaw, S. Rahman, P. E. Georghiou and T. Yamato, *New J. Chem.*, 2014, **38**, 6041–6049.
- 34 O. Kasyan, E. R. Healey, A. Drapailo, M. Zaworotko, S. Cecillon, A. W. Coleman and V. Kalchenko, *J. Inclusion Phenom. Macrocyclic Chem.*, 2007, **58**, 127–132.
- 35 O. Kasyan, V. Kalchenko, V. Böhmer and M. Bolte, *Acta Crystallogr., Sect. E: Struct. Rep. Online*, 2007, **63**, o2346–o2348.
- 36 K. Polívková, M. Šimánová, J. Budka, P. Cuřínová, I. Císařová and P. Lhoták, *Tetrahedron Lett.*, 2009, **50**, 6347–6350.



- 37 M. Dudič, P. Lhoták, H. Petříčková, I. Stibor, K. Lang and J. Sýkora, *Tetrahedron*, 2003, **59**, 2409–2415.
- 38 O. Kasyan, I. Thondorf, M. Bolte, V. Kalchenko and V. Böhmer, *Acta Crystallogr., Sect. C: Cryst. Struct. Commun.*, 2006, **62**, o289–o294.
- 39 V. Bhalla, M. Kumar, C. Kabuto, T. Hattori and S. Miyano, *Chem. Lett.*, 2004, **33**, 184–185.
- 40 S.-J. Shi, X.-X. Lv, M. Zhao, J.-P. Ma and D.-S. Guo, *J. Mol. Struct.*, 2017, **1127**, 81–87.
- 41 V. Burilov, A. Valiyakhmetova, D. Mironova, R. Safiullin, M. Kadirov, K. Ivshin, O. Kataeva, S. Solovieva and I. Antipin, *RSC Adv.*, 2016, **6**, 44873–44877.
- 42 T. Sreeja, V. B. Ganga, L. Praveen and R. L. Varma, *Indian J. Chem., Sect. B: Org. Chem. Incl. Med. Chem.*, 2011, **50**, 704–714.
- 43 V. Bhalla, M. Kumar, H. Katagiri, T. Hattori and S. Miyano, *Tetrahedron Lett.*, 2005, **46**, 121–124.
- 44 H. Dvořáková, J. Lang, J. Vlach, J. Sýkora, M. Čajan, M. Himl, M. Pojarová, I. Stibor and P. Lhoták, *J. Org. Chem.*, 2007, **72**, 7157–7166.
- 45 W. Wang, W. Yang, R. Guo and S. Gong, *CrystEngComm*, 2015, **17**, 7663–7675.
- 46 A. Habashneh, C. R. Jablonski, J. Collins and P. E. Georghiou, *New J. Chem.*, 2008, **32**, 1590–1596.
- 47 S. Bouhroum, J. S. Kim, S. W. Lee, P. Thuéry, G. Yap, F. Arnaud-Neu and J. Vicens, *J. Inclusion Phenom. Macrocyclic Chem.*, 2008, **62**, 239–250.
- 48 K. U. M. Rao, T. Kimuro, M. Yamada, Y. Kondo and F. Hamada, *Heterocycles*, 2015, **91**, 989–1000.
- 49 T. Yamato, C. Pérez-Casas, A. Yoshizawa, S. Rahman, M. R. J. Elsegood and C. Redshaw, *J. Inclusion Phenom. Macrocyclic Chem.*, 2009, **63**, 301–308.
- 50 S. N. Podyachev, B. M. Gabidullin, V. V. Syakaev, S. N. Sudakova, A. T. Gubaidullin, W. D. Habicher and A. I. Kononov, *J. Mol. Struct.*, 2011, **1001**, 125–133.
- 51 V. Št'astný, I. Stibor, H. Petříčková, J. Sýkora and P. Lhoták, *Tetrahedron*, 2005, **61**, 9990–9995.
- 52 P. Lhoták, M. Dudič, I. Stibor, H. Petříčková, J. Sýkora and J. Hodačová, *Chem. Commun.*, 2001, **8**, 731–732.
- 53 L.-L. Liu, L.-S. Chen, J.-P. Ma and D.-S. Guo, *Acta Crystallogr., Sect. E: Struct. Rep. Online*, 2011, **67**, o1110–o1111.
- 54 L.-J. Zhang, L.-L. Liu, Q.-K. Liu and D.-S. Guo, *Acta Crystallogr., Sect. E: Struct. Rep. Online*, 2012, **68**, o1353–o1354.
- 55 P. Lhoták, J. Morávek, T. Šmejkal, I. Stibor and J. Sýkora, *Tetrahedron Lett.*, 2003, **44**, 7333–7336.
- 56 G. Mislin, E. Graf, M. W. Hosseini, A. D. Cian and J. Fischer, *Tetrahedron Lett.*, 1999, **40**, 1129–1132.
- 57 N. Morohashi, N. Iki, C. Kabuto and S. Miyano, *Tetrahedron Lett.*, 2000, **41**, 2933–2937.
- 58 G. Mislin, E. Graf, M. W. Hosseini, A. D. Cian and J. Fischer, *Chem. Commun.*, 1998, **13**, 1345–1346.
- 59 L. Hu, Y. Liu, J.-P. Ma and D.-S. Guo, *Acta Crystallogr., Sect. E: Struct. Rep. Online*, 2009, **65**, o385–o386.
- 60 P. Lhoták, M. Himl, I. Stibor, J. Sýkora, H. Dvořáková, J. Lang and H. Petříčková, *Tetrahedron*, 2003, **59**, 7581–7585.
- 61 L. Liu, K. Huang and C. G. Yan, *J. Inclusion Phenom. Macrocyclic Chem.*, 2010, **66**, 349–355.
- 62 V. V. Syakaev, S. N. Podyachev, A. T. Gubaidullin, S. N. Sudakova and A. I. Kononov, *J. Mol. Struct.*, 2008, **885**, 111–121.
- 63 X. Li, S.-L. Gong, W.-P. Yang, Y.-Y. Chen and X.-G. Meng, *Tetrahedron*, 2008, **64**, 6230–6237.
- 64 X. Li, S.-L. Gong, Y.-F. Liu, Q. Zheng and Y.-Y. Chen, *Acta Crystallogr., Sect. E: Struct. Rep. Online*, 2007, **63**, o2097–o2098.
- 65 B.-T. Zhao, Z. Zhou and Z.-N. Yan, *J. Chem. Sci.*, 2009, **121**, 1047–1052.
- 66 D.-S. Guo, Z.-P. Liu, J.-P. Ma and R.-Q. Huang, *Tetrahedron Lett.*, 2007, **48**, 1221–1224.
- 67 S. N. Podyachev, S. N. Sudakova, B. M. Gabidullin, V. V. Syakaev, A. T. Gubaidullin, W. Dehaen and A. I. Kononov, *Tetrahedron Lett.*, 2012, **53**, 3135–3139.
- 68 T. Yamato, C. Pérez-Casas, S. Rahman, Z. Xi, M. R. J. Elsegood and C. Redshaw, *J. Inclusion Phenom. Macrocyclic Chem.*, 2007, **58**, 193–197.
- 69 C. Pérez-Casas, H. Höpfl and A. K. Yatsimirsky, *J. Inclusion Phenom. Macrocyclic Chem.*, 2010, **68**, 387–398.
- 70 X.-L. Ni, X. Zeng, D. L. Hughes, C. Redshaw and T. Yamato, *Supramol. Chem.*, 2011, **23**, 689–695.
- 71 H. Tomiyasu, J.-L. Zhao, X.-L. Ni, X. Zeng, M. R. J. Elsegood, B. Jones, C. Redshaw, S. J. Teat and T. Yamato, *RSC Adv.*, 2015, **5**, 14747–14755.
- 72 Q. Sun, L. Mu, X. Zeng, J. Zhao, T. Yamato and J. Zhang, *Sci. China: Chem.*, 2015, **58**, 539–544.
- 73 Y. Fu, X. Zeng, L. Mu, X.-K. Jiang, M. Deng, J.-X. Zhang and T. Yamato, *Sens. Actuators, B*, 2012, **164**, 69–75.
- 74 B.-T. Zhao, L. Wang and B.-X. Ye, *Acta Chim. Sin.*, 2007, **65**, 1663–1669.
- 75 F. Hamada, M. Yamada, Y. Kondo, S. Ito and U. Akiba, *CrystEngComm*, 2011, **13**, 6920–6922.
- 76 M. Yamada, Y. Ootashiro, Y. Kondo and F. Hamada, *Tetrahedron Lett.*, 2013, **54**, 1510–1514.
- 77 M. Yamada, R. Kanazawa and F. Hamada, *CrystEngComm*, 2014, **16**, 2605–2614.
- 78 M. Yamada and F. Hamada, *Cryst. Growth Des.*, 2015, **15**, 1889–1897.
- 79 J. Lukášek, S. Böhm, H. Dvořáková, V. Eigner and P. Lhoták, *Org. Lett.*, 2014, **16**, 5100–5103.
- 80 O. Kunderát, V. Eigner, P. Cuřínová, J. Kroupa and P. Lhoták, *Tetrahedron*, 2011, **67**, 8367–8372.
- 81 F. Botha, S. Böhm, H. Dvořáková, V. Eigner and P. Lhoták, *Org. Biomol. Chem.*, 2014, **12**, 5136–5143.
- 82 P. Lhoták, L. Kaplánek, I. Stibor, J. Lang, H. Dvořáková, R. Hrabal and J. Sýkora, *Tetrahedron Lett.*, 2000, **41**, 9339–9344.
- 83 P. Lhoták, M. Himl, I. Stibor and H. Petříčková, *Tetrahedron Lett.*, 2002, **43**, 9621–9624.
- 84 J. Kroupa, I. Stibor, M. Pojarová, M. Tkadlecová and P. Lhoták, *Tetrahedron*, 2008, **64**, 10075–10079.
- 85 I. S. Antipin, I. I. Stoikov, A. T. Gubaidullin, I. A. Litvinov, D. Weber, W. D. Habicher and A. I. Kononov, *Tetrahedron Lett.*, 1999, **40**, 8461–8464.



- 86 S. Dong, W. Zhu, D. Yuan and X. Yan, *Acta Crystallogr., Sect. C: Cryst. Struct. Commun.*, 2002, **58**, o376–o377.
- 87 C. Desroches, S. Parola, F. Vocanson, M. Perrin, R. Lamartine, J.-M. L  toff   and J. Bouix, *New J. Chem.*, 2002, **26**, 651–655.
- 88 C. Desroches, S. Parola, F. Vocanson, N. Ehlinger, P. Miele, R. Lamartine, J. Bouix, A. Eriksson, M. Lindgren and C. Lopes, *J. Mater. Chem.*, 2001, **11**, 3014–3017.
- 89 S. P. Singh, A. Chakrabarti, H. M. Chawla and N. Pant, *Tetrahedron*, 2008, **64**, 1983–1997.
- 90 M.   im  nov  , H. Dvoř  kov  , I. Stibor, M. Pojarov   and P. Lhot  k, *Tetrahedron Lett.*, 2008, **49**, 1026–1029.
- 91 C. Desroches, V. G. Kessler and S. Parola, *Tetrahedron Lett.*, 2004, **45**, 6329–6331.
- 92 W.-N. Xu, J.-M. Yuan, Y. Liu, J.-P. Ma and D.-S. Guo, *Acta Crystallogr., Sect. C: Cryst. Struct. Commun.*, 2008, **64**, o349–o352.

